



East African Journal of Forestry & Agroforestry

eajfa.eanso.org

Volume 7, Issue 1, 2024

Print ISSN: 2707-4315 | Online ISSN: 2707-4323

Title DOI: <https://doi.org/10.37284/2707-4323>



EAST AFRICAN
NATURE &
SCIENCE
ORGANIZATION

Original Article

Historical Trend Analysis and Future Projections of Rainfall in Amhara, Ethiopia

Antensay Mekoya^{1*}, Moges Molla², Mulatu Workneh³ & Tewachew Worku¹

¹ Ethiopian Forestry Development Bahir Dar Center, P. O. Box 2128, Bahir Dar, Ethiopia.

² Ethiopian Forestry Development Hawassa Center, P. O. Box 1832 Hawassa, Ethiopia.

³ Ethiopia Meteorology Institute Addis Ababa, P. O. Box 1090, Addis Ababa, Ethiopia.

* Author for Correspondence ORCID ID: <https://orcid.org/0000-0002-2895-4581>; email: antensaymekoya@yahoo.com

Article DOI: <https://doi.org/10.37284/eajfa.7.1.1760>

Date Published: ABSTRACT

18 February 2024

Keywords:

Climatology,
Climate Change,
CORDEX Project
GCMs,
CMIP5 in RCP
Scenarios.

Understanding rainfall trends & projections is essential for water resource management. This study showed historical (1981-2020) and future (2021-2100) rainfall amounts and trends across 71 grid points separated by 0.44° in Amhara and Amhara's five rainfall regimes (A3, A4, A5U, A5L, A6). Ground and satellite merged historical data from Ethiopia Meteorology Institute (EMI) and the Rossby Centre Regional Atmospheric Model (RCA) forced by an ensemble of the best-performed Global Circulation Models (GCMs) in Amhara, HadGEM2-ES of UK and MPI-ESM-LR of Germany, in three Representative Concentration Pathway (RCP) scenarios, RCP2.6, RCP4.5, and RCP8.5 from CORDEX project were the basis of dataset. Amhara's annual, seasonal, and monthly historical rainfall trends mostly increased. During Jun-Sep (Kiremt), lower rainfall receiving regimes (A6, A5L, A5U) had a significant increasing trend (~ 4 mm/year), while wetter regimes (A3 & A4) had a non-significant increasing (< 1 mm/year) and decreasing (~ -0.5 mm/year) trends, respectively. Generally, compared to the climatology, the annual and Kiremt rainfall in Amhara is projected to increase in the near-term (2021-2040) and mid-term (2041-2060) and decrease in the long-term (2081-2100); Oct-Jan (Bega) rainfall is projected to increase in all future terms and all RCP scenarios while Feb-May (Belg) rainfall will be abrupt.

APA CITATION

Mekoya, A., Molla, M., Workneh, M. & Worku, T. (2024). Historical Trend Analysis and Future Projections of Rainfall in Amhara, Ethiopia *East African Journal of Forestry and Agroforestry*, 7(1), 19-49. <https://doi.org/10.37284/eajfa.7.1.1760>

CHICAGO CITATION

Mekoya, Antensay, Moges Molla, Mulatu Workneh and Tewachew Worku. 2024. "Historical Trend Analysis and Future Projections of Rainfall in Amhara, Ethiopia" *East African Journal of Forestry and Agroforestry* 7 (1), 19-49. <https://doi.org/10.37284/eajfa.7.1.1760>

HARVARD CITATION

Mekoya, A., Molla, M., Workneh, M. & Worku, T. (2024), "Historical Trend Analysis and Future Projections of Rainfall in Amhara, Ethiopia", *East African Journal of Forestry and Agroforestry*, 7(1), pp. 19-49. doi: 10.37284/eajfa.7.1.1760.

IEEE CITATION

A., Mekoya, M., Molla, M., Workneh & T., Worku "Historical Trend Analysis and Future Projections of Rainfall in Amhara, Ethiopia", *EAJFA*, vol. 7, no. 1, pp. 19-49, Feb. 2024.

MLA CITATION

Mekoya, Antensay, Moges Molla, Mulatu Workneh & Tewachew Worku. "Historical Trend Analysis and Future Projections of Rainfall in Amhara, Ethiopia". *East African Journal of Forestry and Agroforestry*, Vol. 7, no. 1, Feb. 2024, pp. 19-49, doi:10.37284/eajfa.7.1.1760

INTRODUCTION

Research Rationale

Climate Change and Its Impact

Climate has the main effect on the biophysical resources of the Earth, and its change will affect ecosystems and biodiversity. Since the last few decades, weather and climate variability and climate change have become scientific, social, political, and economic concerns of many countries worldwide. Climate change has been the main threat to the global food system (Jabal et al., 2022), particularly in developing countries. Like most African countries, developing countries are vulnerable to adverse impacts of climate change and variability because they have low adaptive capacity and high exposure as their economies rely mainly on agriculture. Among African regions, East Africa is the most vulnerable (Gebrechorkos et al., 2018; Zegeye et al., 2022; Gedefaw, 2023). In East Africa, agriculture contributes 30-50% of gross domestic product (GDP) and >80% of livelihood (FAO, 2014). Ethiopia follows an agriculture-led industrialization economic policy where agriculture is the source of approximately 85%, >80%, and 50% of the annual total import/export revenue, labor force, and GDP, respectively (Cochrane & Vercillo, 2019). Since African countries, particularly the sub-Sahara countries, are mainly dependent on rain-fed agriculture, their climate change coping capacities are poor (IPCC, 2019). Ethiopia, one of the east or Greater Horn of Africa (GHA) or sub-Saharan countries, has a complex climate and topography (Bekele-Biratu et al., 2018). The complex topography is evident because Africa's most pronounced mountain systems are found in Ethiopia (Haile et al., 2006), accounting for more than 70% of African mountains (Azadi et al., 2020). The complex topography is associated with Ethiopia's complex climate, where high and low rainfall amounts in

receiving areas are found within a few kilometers of each other.

Rainfall in Ethiopia

Rainfall or precipitation is one of the crucial climatic elements or meteorological parameters in determining the climate of a place; its change directly or indirectly affects different hydro-climate systems. Ethiopia's economy, which is mainly dependent on natural rain-fed agriculture, where irrigation accounts for <1.1% of the total cultivated land (Bewket & Conway, 2007), is negatively impacted by rainfall fluctuations (Belay et al., 2019). For example, a 10% decrease in seasonal rainfall of Ethiopia, compared to the climatology, translates to a 4.4% decrease in crop production (Braun, 1991), and a significant decreasing rainfall amount may lead to meteorological drought (Kamalanandhini & Annadurai, 2021). Because Ethiopia has less climate change adaptation potential, without proper management options with the aid of meteorological forecasts, a significant decrease in rainfall amount during the main rainy season exacerbated by late onset and untimely cessation of rainfall and higher evapotranspiration and frost occurrence may cause both meteorological and agricultural drought as well as famine in Ethiopia.

Climate change and extremes have adversely affected food security, particularly in rain-fed agricultural production systems (Behailu et al., 2021). The rainfall in northern Ethiopia is erratic, with a short Length of Growing Period (LGP) and frequent late onset and early end (cessation), negatively impacting agriculture (crop growth and yield, forage, cattle, etc) (Berhane et al., 2020). Due to climate change, the seasonal and annual rainfall amount and distribution of rainfall amount may change significantly, negatively impacting a country's agriculture, food security, water resources, and other socio-economic activities. In Ethiopia, seasons are traditionally divided into four (Jun-Aug: Meher or "Kiremt," Sep-Nov:

Belg, Dec-Feb: winter or “Bega,” Mar-May: Spring; also refer to Musayev et al. (2021). However, in this article, the classification of seasons adopted by most of the scientific community, including the research reports of the Ethiopian Meteorology Institute (EMI), formerly called the National Meteorological Agency of Ethiopia (NMA, 1996), which divided seasons and rainfall regimes of Ethiopia into three (Bekele-Biratu et al., 2018) was used. Accordingly, the rain during June-September, or “Kiremt” season, is the major rainy season (wet season) in most parts of Ethiopia except the southeast and south lowlands. February-May or “Belg” is the second rainy season (second wet season) in the central, northeast, and the highlands of the east and south of Ethiopia; it is also the main rainy season in southeast and south lowlands of Ethiopia (Bekele-Biratu et al., 2018). October-January, or “Bega,” is a dry season in most parts of Ethiopia. The three regimes of Ethiopia are mono-modal (having one main rainy season in a year), bi-modal-I (having one main and secondary/additional rainy season in a year), and bi-modal-II or diffused/quasi-bimodal rainfall patterns. Generally, the climatology of Ethiopia using daily rainfall data from NMA during 1980-2010 showed that the western half, excluding the southern and some central parts of Ethiopia, received above 1000 mm annual total rainfall while the lowlands of vast areas in southeast and some areas in northeast received below 500 mm (Bekele-Biratu et al., 2018).

Rainfall and its Trend and Projection in Amhara, Ethiopia

The rainfall of Amhara regional state of Ethiopia is dominated by monomodal or unimodal rainfall pattern; however, a few areas in the eastern Amhara or some areas in regimes A5L and A6 show bimodal or nearly bimodal rainfall pattern (Mekoya & Molla, 2024). In Ethiopia, climate change, particularly changes in rainfall and air temperature, is already manifested; however, the amount and distribution of the change at regional levels and its statistical associations with crop production were not well studied (Ayalew et al., 2012b; Bewket & Conway, 2007). This study

showed the historical (1981-2020) and climate model outputs of future (2021-2100) temporal and spatial rainfall amount trends of the Amhara regional state of Ethiopia.

Climate models are essential for projecting global or regional future climate, and they have been used in climate change adaptation and mitigation strategies (Luhunga et al., 2018). For climate projection, Global Climate Models (GCMs) have been widely used (Yimer et al., 2022), whereas Regional Climate Models (RCMs) are more suitable in mountainous and coastal regions and at regional or small-scales (Kassahun et al., 2023). Historical and future climate data, both GCMs and RCMs outputs, of the Coupled Model Intercomparison Project phase 5 (CMIP5), which used the Representative Concentration Pathway (RCP) scenarios, can be freely downloaded from the Coordinated Regional Climate Downscaling Experiment (CORDEX) project sponsored by the World Climate Research Programs. Determining the most appropriate RCMs is crucial to confidently evaluate the impacts of climate change on agriculture and water resources in regions with complex topography like Ethiopia (Yimer et al., 2022). Selecting the best climate model for a given area is crucial because not all climate models are equally relevant in all areas (Kassahun et al., 2023). Using the Rossby Centre Regional Atmospheric Model version 1 (RCA4_v1) RCM, (Mekoya & Molla, 2024) studied the performance of CORDEX GCMs, and they found that the HadGEM2-ES (of UK) and MPI-ESM-LR (of Germany) GCMs were the best in projecting the rainfall of Amhara, Ethiopia. Ensembles of the two best-performed GCMs were used throughout this study. However, it is worth understanding that models cannot perfectly reproduce the real world’s climate reality even with perfect boundary conditions/forcing due to model bias (Van Vooren et al., 2019).

Relevance of the Study

Reliable rainfall trends and projection information are essential in many socio-economic development applications, such as agriculture, hydro-power generation, water resources

development, and forestry, for monitoring drought and disaster management, floods, and ecosystems (Belay et al., 2019). As rainfall is the most important meteorological element, it directly affects the socio-economic and food security conditions of a society depending on rain-fed agriculture. Because human-induced climate variability and change have detrimental effects on socio-economic activities such as livelihood, food security, and health (Budusa-Ware et al., 2023), the rainfall trend and projection information in the Amhara regional state of Ethiopia will be crucial for implementing climate change adaption and mitigation strategies in the region. Thus, documented spatiotemporal historical trends and future projections of the rainfall amount of the Amhara regional state of Ethiopia are useful information inputs in policy making and water resources planning and management.

MATERIALS AND METHODS

Study Area

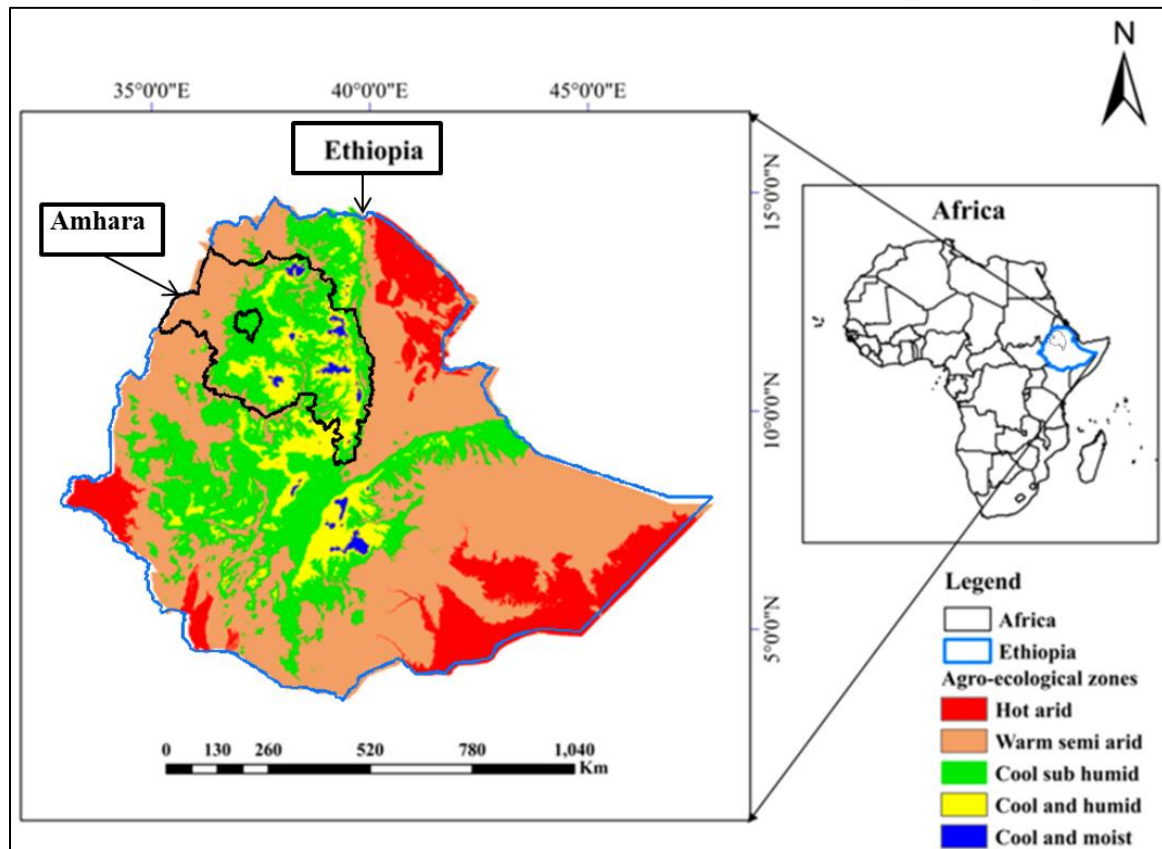
The study area is Amhara or Amhara National Regional State of Ethiopia (ANRSE) (see Fig. 1-2), located in the north western and north-central parts of Ethiopia between latitude 8.8° & 13.64° N and longitude 35.2° & 40.04° E. Amhara region which is divided into 10 administrative zones consisting of 105 Woredas (sub-districts), is the second most populous region in Ethiopia (25% of the Ethiopian population resides in Amhara). As of 2023, the region had 13 administrative zones, with Gonder and Gojam having four and three distinct sub-districts, respectively. It had a population of 21.1 million in 2017 (UNICEF, 2018; Hailu et al., 2018). Amhara has enormous water and livestock resources, 90% of which are

in rural parts engaged in subsistence crop and livestock agriculture activities (CSA, 2007). It has a total area of about 170,000 km², of which about 156,000 km² is mountainous (Sisay *et al.*, 2016; Birara et al., 2018). Its altitude ranges from 700 m in the eastern part to 4620 m a.s.l. (at Ras Dashen, the highest peak in Ethiopia) in the north-west (Birara et al., 2018).

Dividing a country or a state into climate boundaries instead of following political or state boundaries will make climate studies more effective. Thus, in this study, the Amhara regional state is further subdivided into five rainfall shape regimes (A3, A4, A5L, A5U, and A6) as precisely represented in Fig. 2. In Ethiopia, the rainfall of a day is the total rainfall amount from that day at 7 am until the next day at 7 am; the measurement is taken or recorded on the next day at 7 am. A wet day or rainy day is defined as a day with ≥ 0.1 mm of precipitation (Harris et al., 2020). This study defines a rainy day as a day with greater than 0.1 mm of rain in a day or within 24 hours (Seleshi & Zanke, 2004). In warm tropical regions like Ethiopia, the definition of rainy days by Seleshi and Zanke (2004) is preferred due to the availability of high evapotranspiration.

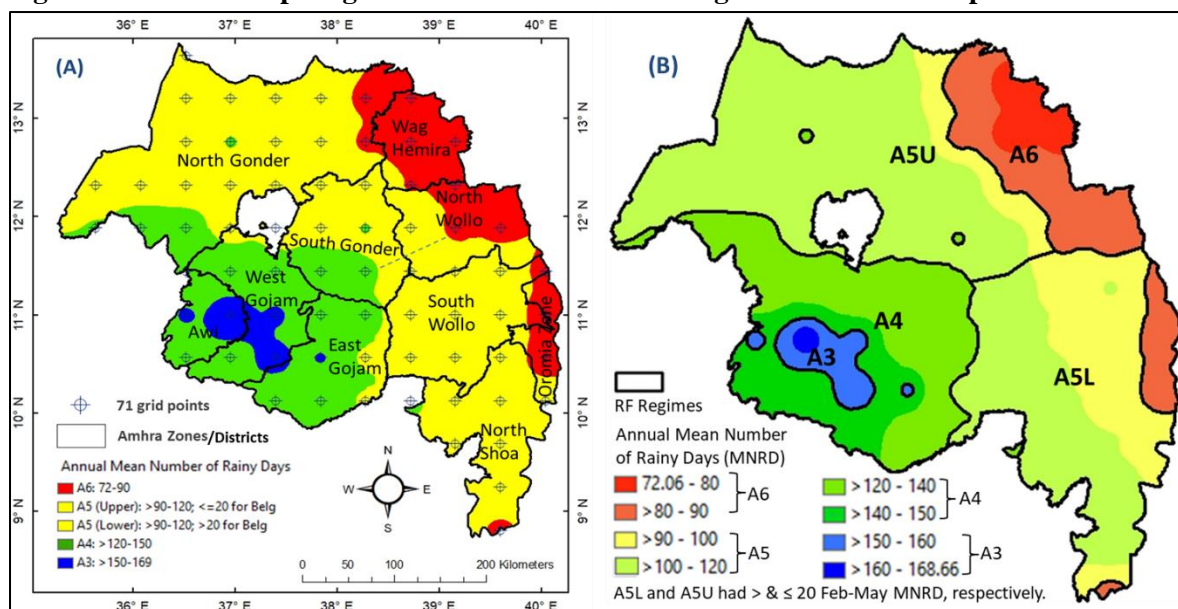
Based on altitude variations, the climate of the Amhara region is traditionally divided into three: 1) hot zone or 'Kola,' < 1500 m a.s.l.; covers 31% of the region. 2) warm zone or 'Woyina Dega' (1500 – 2500 m a.s.l.); covers 44% of the region. 3) The cold zone or 'Dega' (2500 - 4620 m a.s.l.) covers 25% of the region (Ayalew et al., 2012a). From 1981 to 2020, the region's monthly mean maximum, minimum, and air temperatures were 26.7, 12.5, and 19.6 °C, respectively.

Figure 1: Study Area: Location of Amhara in Agro-ecological Zones map of Ethiopia



Source: (Wubaye et al., 2023)

Figure 2: Rainfall shape regimes of Amhara National Regional State of Ethiopia



Source: (Mekoya & Molla, 2024)

Note: Since 2023, Amhara National Regional State of Ethiopia (ANRSE) has been divided into 22 districts or Zones. However, this study has not used the newly modified map of ANRSE that includes the Wolkait-Tsegele district (north of North Gondar) and Raya

district (north of North Wollo and east of Wag Hamira).

Data

After preparing the base map of the Amhara National Regional State of Ethiopia (ANRSE) (see Fig. 1-2), various kinds of data were collected for the study period from 1980 to 2100 which is divided into historical (1980-2020) and future (2021-2100) periods. Historical climate data was obtained from the Ethiopia Meteorological Institute (EMI), formerly the National Meteorological Agency (NMA) of Ethiopia, from over 180 meteorological stations recording rainfall. However, all the stations do not record air temperature; only a few record relative air humidity, wind speed, sunshine hour duration, solar radiation, air pressure, etc. According to (Sisay et al., 2017), full daily climate data of Amhara can also be freely accessed for the period 1979- 2010 from <ftp://palantir.boku.ac.at/Public/ClimateDataEthiopia>.

For the historical period (1980-2021), station and satellite merged daily rainfall data for seventy-one grid points enclosed within ANRSE, each separated by 0.44° (48.88 km), which was the basis of data analysis. Other open access meteorological datasets such as CRU TS4.07 or CRU TS4.06 (https://crudata.uea.ac.uk/cru/data/hrg/cru_ts_4.06/), climate forecast system reanalysis (CFSR) (<https://globalweather.tamu.edu/>), Terra Climate (<https://www.climatologylab.org/terraclimate.html>), MSWX (www.gloh2o.org/mswx/), etc can be used after bias-correction to check the accuracy (goodness of fit) of the data used.

The future (2021-2100) monthly rainfall amount data was downloaded from the Coordinated Regional Climate Downscaling Experiments (CORDEX) project for Africa (AFR-44) (<https://climate4impact.eu/impactportal/data/esgfsearch.jsp#>) for the most reliable GCMs for projecting rainfall of ANRSE namely HadGEM2-ES of UK and MPI-ESM-LR of Germany (Mekoya & Molla, 2024). The above two driving

GCMs were downloaded using the Rossby Centre Regional Atmospheric Model version 1 (RCA4_v1) Regional Climate Model (RCM) for ensemble r1i1p1 (r1 = 1 ensemble member; i1 = 1 initialization state; p1, 1 physical parameterization) (supplementary materials of Herger et al., 2018; Grose et al., 2023; Demaeyer et al., 2022) for three Representative Concentration Pathways (RCP2.6, RCP4.5, and RCP8.5) scenarios from Coupled Model Inter Comparison Project phase 5 (CMIP5).

Methods

Linear regression analysis (Eq. 1) with students' t-tests was used for rainfall amount trend analysis. To test the significance of the slope (Eq. 2) and correlation coefficient (Eq. 4), the statistical t-test (Eq. 5) was applied. The least square method was used to fit the data that minimizes the sum of the squared residuals. The slope (b) and Intercept (a) of the least squares line are given by Eq. 2 and Eq. 3, respectively.

$$y_i = bx_i + a \quad (1)$$

where y_i is the dependent variable (rainfall amount), x_i is the independent variable (years from $i = 2021$ to 2100 for future rainfall data analysis and numbers from $i = 1$ to 40 correspond to the years from 1981 to 2020 for historical trend analysis), b is the slope or trend, a is the y-intercept when x is zero. Positive (negative) values of b indicate increasing (decreasing) trends, and a larger (smaller) value of b indicates a stronger (weaker) trend of y . To determine the statistically significant (for $p < 0.05$ used in this study) linear trends, (Huang & Chen, 2011) calculated the statistical variable T as given below (see Eq. 6). Then, the comparison of the T values with the p -values obtained with a Student's t-test was used to determine the significance level of the linear regression trend (Sun et al., 2017; Xu et al., 2021).

$$b = \frac{SS_{xy}}{SS_{xx}} = \frac{\sum_{i=1}^N (x_i - \bar{x})(y_i - \bar{y})}{\sum_{i=1}^N (x_i - \bar{x})^2} \quad (2)$$

$$a = \bar{y} - b\bar{x} \quad (3)$$

$$r = \frac{\sum_{i=1}^n (x_i - \bar{x})(y_i - \bar{y})}{\sqrt{[\sum_{i=1}^n (x_i - \bar{x})^2] \sum_{i=1}^n (y_i - \bar{y})^2}} \quad (4)$$

$$t = \frac{r\sqrt{N-2}}{\sqrt{1-r^2}} \quad (5)$$

$$T = t \frac{1}{n-2} = \frac{r}{\sqrt{(1-r^2)(n-2)}} \quad (6)$$

Where SS_{xy} is the sum of the cross-products; SS_{xx} is the sum of the squares for the variable x ; x_i is the i^{th} time (year) for the constituent being evaluated; y_i is the i^{th} rainfall amount for the constituent being evaluated; N is the total number of observations; \bar{x} and \bar{y} denote the mean for x_i and y_i for the entire period of the evaluation; t is the student's test; and r is the correlation coefficient between y & x .

Trend analysis was performed using Eq. 2-6 throughout this study. For example, Eq. 2 can be equivalently applied using the simple formula in the Microsoft Excel workbook: “=SLOPE (known_y's, known_x's,” which returns the slope of the linear regression line through the given data points. To test the significance of the correlation, the built-in function ‘cor-test’ using the non-parametric method = “Kendall” was used in the RStudio platform. Also, using the result of Eq. 5, the formula: ‘p-value = DIST (x,deg_freedom, tails)’ in Microsoft Excel is used; here, x is the t value, $\text{deg_freedom} = N-2$; N is the sample size (40 years from 1981 to 2020 and 80 years from 2021-2100 for historical and future data, respectively). The results of the two methods were similar.

Another two trend tests were also used to test and validate this study's accuracy. The first was the Mann-Kendall (MK) trend test. The Mann-Kendall (MK) test has been used as the standard trend test in many studies. The Mann-Kendall (MK) trend test is used to test whether the null hypothesis (H_0) and observations are randomly ordered in time or whether the alternative

hypothesis (H_1), which is an increasing or decreasing monotonic trend in time series, is true. In the MK trend test, the determining Sen's slope (S) and significant (Z) statistics were calculated using (Salas, 1993) as described in Alemu & Bawoke (2020) (see Eq. 10-14 in Alemu & Bawoke (2020) and Jain et al. (2013) (see Eq. 3-7 in Jain et al. (2013).

Positive and negative values of Z indicate increasing and decreasing trends, respectively, and S is the magnitude of the trend. This method is applied in the R or RStudio platform using the “trend” package and “sens. slope” and or “mk. test” function(s). The second trend analysis method separated the long-term observations into two equal parts. If the number of observations is an odd number, the data of the first year (in the time series) shall be omitted to make it an even number of total observations (N). On a coordinate system, the first-half (the older time series) X_i : $i = 1, 2, 3, \dots, n$ is placed on the X-axis and the second-half (the recent time series) Y_i : $i = 1, 2, 3, \dots, n$ is placed in Y-axis where $n = N/2$ is number of observations in the first-half (older) or second-half (recent) subseries class (see *Appendix 14* for the template of (Terefe et al., 2022). In a scatter plot, if the time series data accumulate on a 45° or 1:1 straight trend line that passes through the origin (0,0), it indicates no trend. The trend increases or decreases if most data are placed/collected above or below the line. The formula for this innovative trend analysis (ITA) trend indicator (ϕ) is given in Eq. 7 (modified after Şen (2012)).

$$\phi = \frac{f}{n} \sum_{i=1}^n \frac{(Y_i - X_i)}{\mu} \quad (7)$$

Where μ is the mean or average value of the first-half subseries class (X_i) data and ϕ , $n = N/2 = 40/2 = 20$, and Y_i are as defined before, and f is a multiplying factor. To increase the trend magnitude to have a similar scale with the above two trend tests, $f = 73$ (or $f = 80.08$) was used; theoretical $f = 2n$ may be assumed. A positive, zero, and negative value of ϕ indicates increasing, no trend, and decreasing trend, respectively, and

scatter points closest to 45° indicate the trend is non-significant.

The most reliable GCMs for projecting rainfall of Amhara Regional State of Ethiopia (ARSE), namely HadGEM2-ES of the UK and MPI-ESM-LR of Germany (Mekoya & Molla, 2024) was, used for projecting the future rainfall amount for the period 2021-2100. The IPCC (AR6-WGI-Chapter 4) grouped the period 2021-2100 into three in their global climate projection assessment based on the Shared Socio-economic Pathways (SSPs) Scenarios used in the Coupled Model Intercomparison Project Phase 6 (CMIP6): 1) near-term (2021-2040), 2) mid-term (2041-2060), and 4) long-term (2081-2100) (Lee et al., 2021).

The trend and projection results were georeferenced, interpolated, and mapped using ArcGIS 10.8 or R software. The inverse distance weighting (IDW) interpolation method was used for spatial mapping. The general formula for IDW interpolation is formed as a weighted sum of the data, see Eq. 8.

$$Z(S_o) = \sum_{i=1}^N \lambda_i Z(s_i) \quad (8)$$

Where $Z(s_i)$ is the measured value at the i^{th} location, λ_i is an unknown weight depending on the distance between the known and the prediction location, s_o is the prediction location, and N is the number of measured values.

RESULTS AND DISCUSSIONS

Rainfall Climatology

The mean annual rainfall amount of Amhara National Regional State of Ethiopia (ANRSE) was 990.2 mm in 1 m² area. It was equivalent to 168 billion cubic meters (BCM) of rain water over the whole Amhara (990.2 mm * 170,00 km² = 0.9902 m * 170,000 * 10⁶ m² = 1.68 * 10¹¹ m³) (see Appendix 3; also see Figure 5a and Appendix 10 (a) in Supplementary Materials). The rainfall of Amhara is mostly mono-modal, having the highest monthly mean amount in August (279.2 mm) and July (276.4) and generally decreases from July to January and from August to December (see Appendix 3) except for Regimes A5L and A6, where it shows a quasi-bimodal

pattern during March-May. The spatial distribution of mean annual and seasonal (Jun-Sep, Feb-May, and Oct-Jan) total rainfall amounts is shown in Figure 5-8a, respectively. Most areas, particularly the eastern-half of the region, received below the regional mean annual rainfall amount (513-990 mm), while some areas, particularly located in the western-half of the region, received above the regional mean (>990-2113 mm) (Figure 5a). In Bega (Oct-Jan), half of Amhara received below (9-63 mm), and while the rest received above (>63-477 mm), the region's Oct-Jan average (63 mm) as depicted in Figure 6a. In Belg (Feb-May), the northern and southern parts of the region received below (32-126 mm) and above (>126-355 mm) the region's Feb-May average (126 mm), respectively (Figure 7a). In Kiremt (Jun-Sep), which is the main rainy season of Amhara and most of Ethiopia, the eastern and western parts of Amhara received below (191-801 mm) and above (>801-1647 mm) the region's Jun-Sep average (801 mm), respectively (Figure 8a).

Historical Rainfall Trend

The annual, seasonal (Bega, Belg, and Kiremt), and monthly (Jan-Dec) historical trend of rainfall amount in Amhara was mostly increasing during 1981-2020 except in January, March, and December; see Figure 3 and Figure 4a-p as well as Appendix 1-2 and Appendix 10-12(a).

The annual rainfall trend of Amhara and its rainfall regimes was increasing; the increase was significant for Amhara, A5U, and A6 (Figure 3). However, its spatial distribution showed decreasing trends in a few pocket areas, particularly in the southern parts of Awi, West Gojjam, and North Shoa districts (Figure 4m). For example, the annual rainfall trend in Amhara was significantly increasing (SI) in 31 grid points out of a total of 71 grid points (Appendix 2) with a slope (b) = 2.99, p-value = 0.03, and Intercept (a) = 929. Thus, its linear regression equation was $y = 2.99x + 929$; here, y is the annual rainfall amount in Amhara, and x is time ranging from 1 to 40 for the years from 1981 to 2020, respectively.

In the Bega & Belg seasons, the rainfall trend decreased in regimes A5L & A6 (*Figure 3*). None of the Bega & Belg trends was significant in Amhara & its regimes (*Figure 3*), and only a few grid points showed significant spatial trend distribution across the region (*Figure 4n & o*).

In Kiremt, the rainfall trend was significantly increasing except in regime A3; in regime A4, it was decreasing and non-significant (*Figure 3*). Unexpectedly, climatologically low Kiremt rainfall amount receiving areas, regimes A5U (859.7 mm), A5L (672.8 mm), and A6 (509.3 mm) had showed a significant increasing trend (around 4 mm/year) while climatologically high Kiremt rainfall amount receiving areas, regime A3 (1167 mm), particularly Awi district (*Figure 4p*), and regime A4 (978.7 mm) had showed a non-significant increasing (below 1 mm/year) and decreasing (around -0.5 mm/year) trends, respectively (*Figure 3*).

The monthly rainfall trend mainly decreased in Jan, Mar, and Dec and increased during Apr-Nov (see *Figure 3 & Figure 4a-l*). The highest trend of above 1.5 mm/year occurred in August (in regimes A6 & A5L), followed by July (in regimes A5L) (*Figure 3*).

Future Rainfall Projection

Generally, the result indicates that the annual and Kiremt rainfall amount in Amhara will increase in the near- and mid-terms and decrease in the long-term compared to the historical climatology (990 mm for annual and 801 mm for Kiremt) (*Appendix 3*). Bega rainfall is projected to increase in all future terms and all RCP scenarios, while Belg rainfall will be abrupt.

The near-term (2021-2040), mid-term (2041-2060), and long-term (2081-2100) annual and seasonal (Bega, Belg, and Kiremt) mean rainfall amount in Amhara in RCP 2.6, RCP 4.5, and RCP8.5 are projected to be higher (see *Appendix 4-9* and *Appendix 10-13* in Supplementary Materials) except for Belg in near-term in RCP 8.5, in mid-term in RCP 2.6 and RCP 4.5, and in long-term in RCP 4.5 and RCP 8.5 and for Kiremt and annual in long-term in RCP 8.5 as compared

to the historical or climatological mean rainfall amount (see *Appendix 3* in Supplementary Materials). However, the distribution of mean rainfall amount (*Figures 5 & 8b-j*) is projected to be nearly similar as compared to the historical or climatological normal (mean) rainfall amount (*Figures 5 & 8a*). In contrast, the future rainfall distribution in the Bega and Belg seasons (*Figure 6-7b-j*) differs from the historical (*Figure 6-7*). The future mean rainfall amount distribution in the Bega and Belg seasons (*Figures 6 & 8b-j*) will have the same distribution pattern but a different magnitude from the historical mean rainfall amount distribution of the Belg and Bega seasons, respectively (*Figures 7 & 8a*). The future rainfall amounts of Belg and Bega seasons seem exchanged from the sole observation of their distribution pattern; however, their values are actual and can be proved by their corresponding mean rainfall amounts against the historical or climatological normal (126 mm for Belg and 63 mm for Bega) (*Figure 6 & 7a-j*). The mean annual, Kiremt, Belg & Bega future rainfall amount range of Amhara is projected to be 1042-1070, 818-877, 125-137 & 69-90 mm in near-term, 1037-1054, 835-842, 123-126 & 73-87 mm in mid-term, and 973-1050, 760-832, 112-154 & 76-102 mm in long-term, respectively (*Appendix 7-9; Appendix 10-13*)

Figure 1: Annual, Bega (Oct-Jan), Belg (Feb-May), Kiremt (Jun-Sep), and Monthly trends of rainfall in Amhara and its rainfall regimes (A3-A6) during 1981-2020. The asterisk or star, symbol above the bars indicates significant trends.

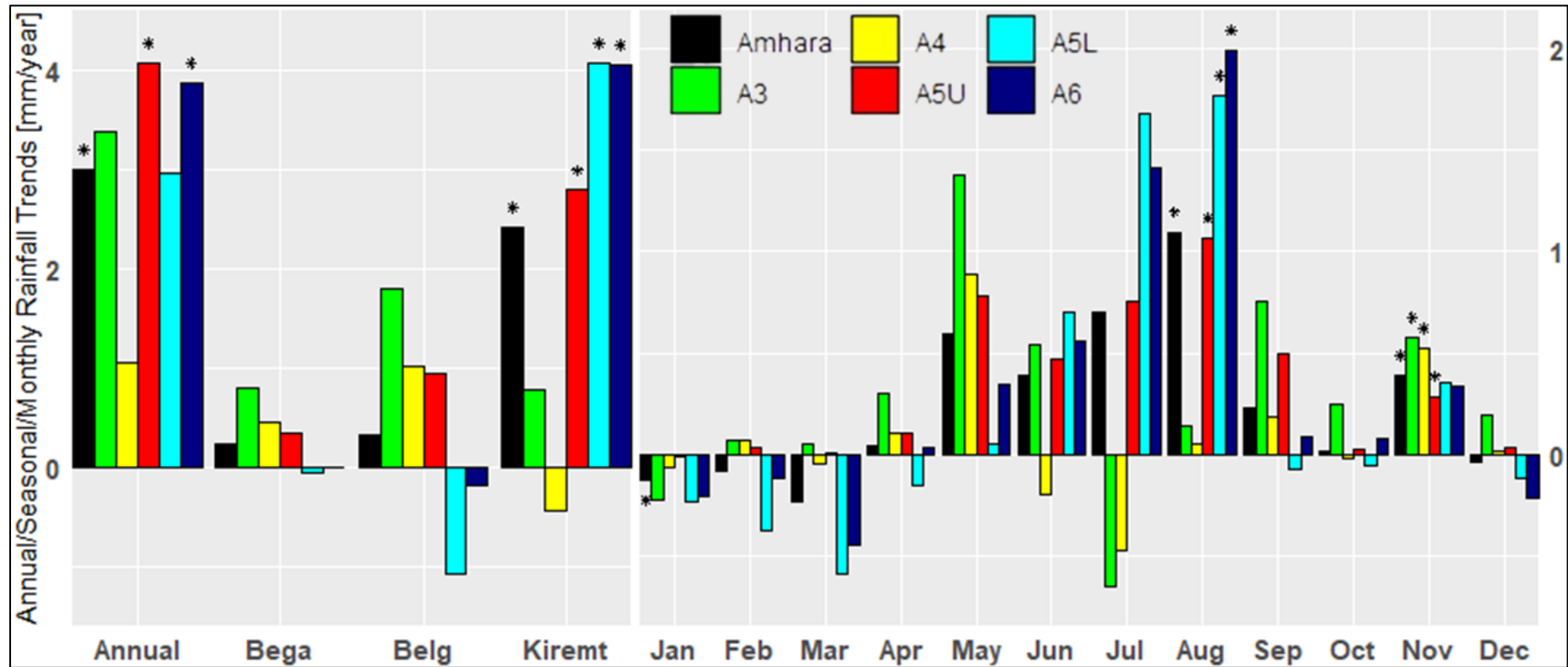


Figure 2: Monthly (a-l), Annual (m), Bega (Oct-Jan) (n), Belg (Feb-May) (o), and Kiremt (Jun-Sep) (p), trends of rainfall in Amhara during 1981-2020. The asterisk or star, symbol in the graph indicates significant trends

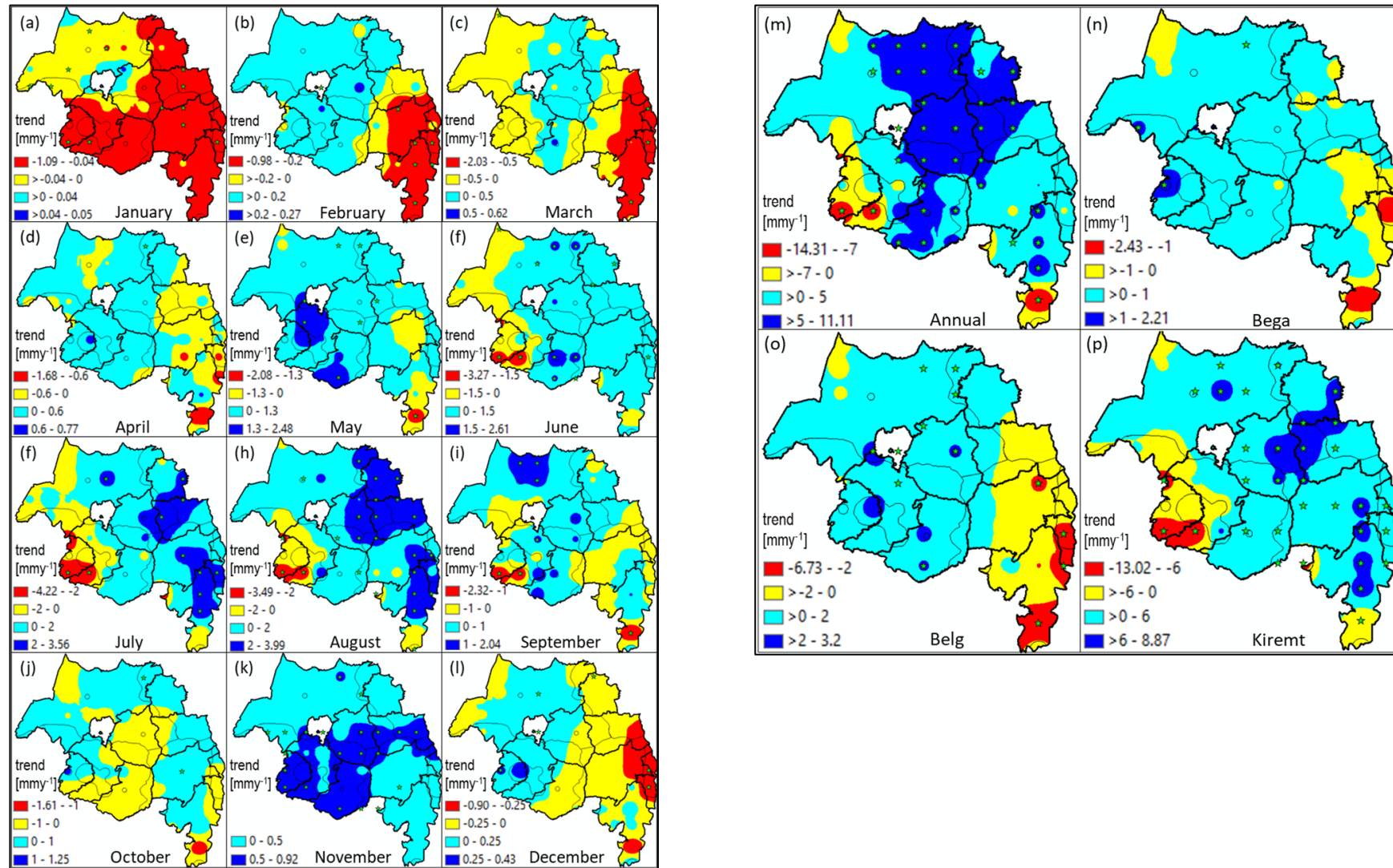


Figure 3: Climatology (a) and Projection (b-j) of average annual total rainfall amount distribution in Amhara, Ethiopia

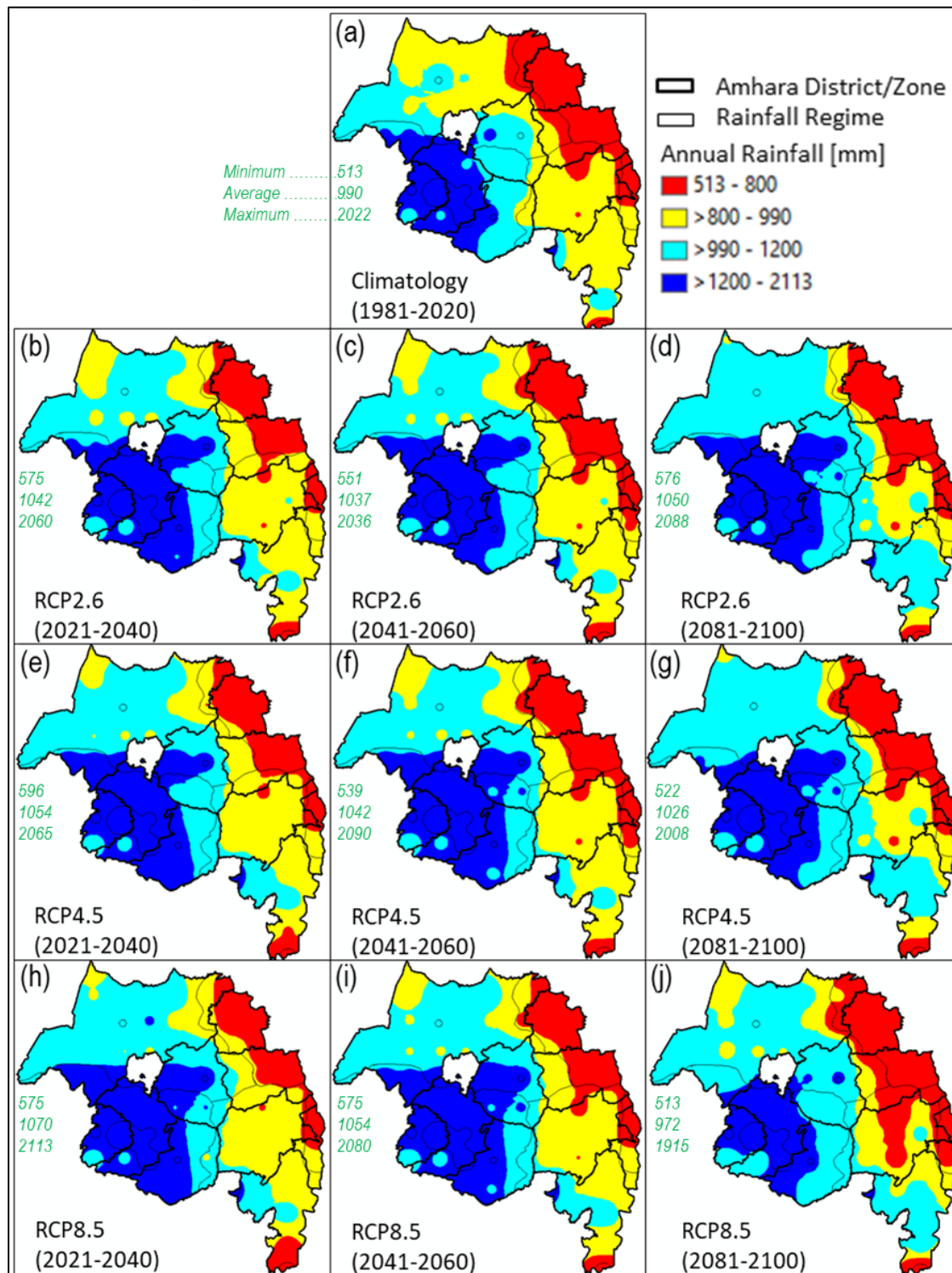


Figure 4: Historical (a) & future (b-j) Bega (Oct-Jan) average rainfall amount in Amhara, Ethiopia

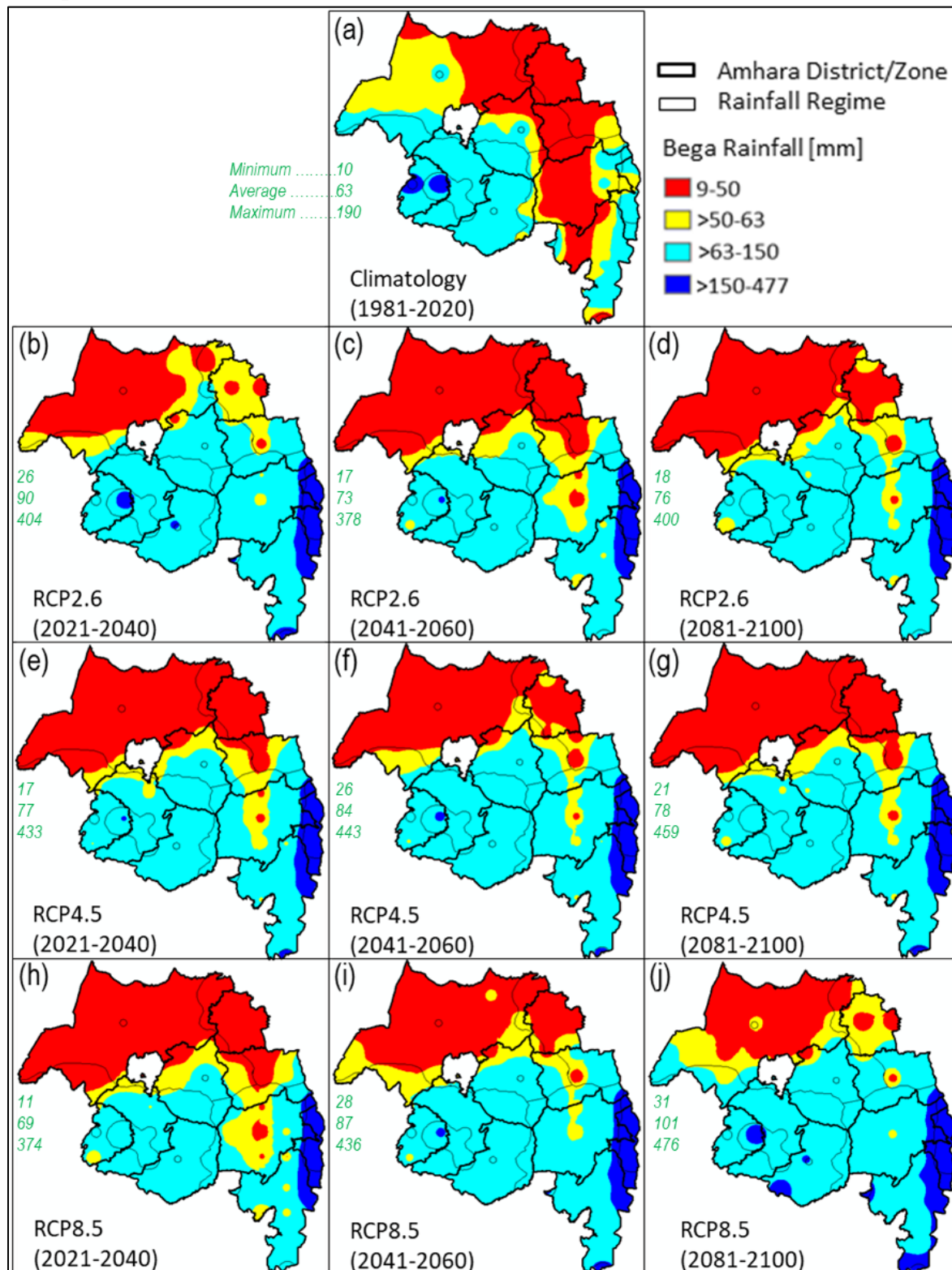


Figure 5: Historical (a) & future (b-j) Belg (Feb-May) average rainfall amount in Amhara, Ethiopia

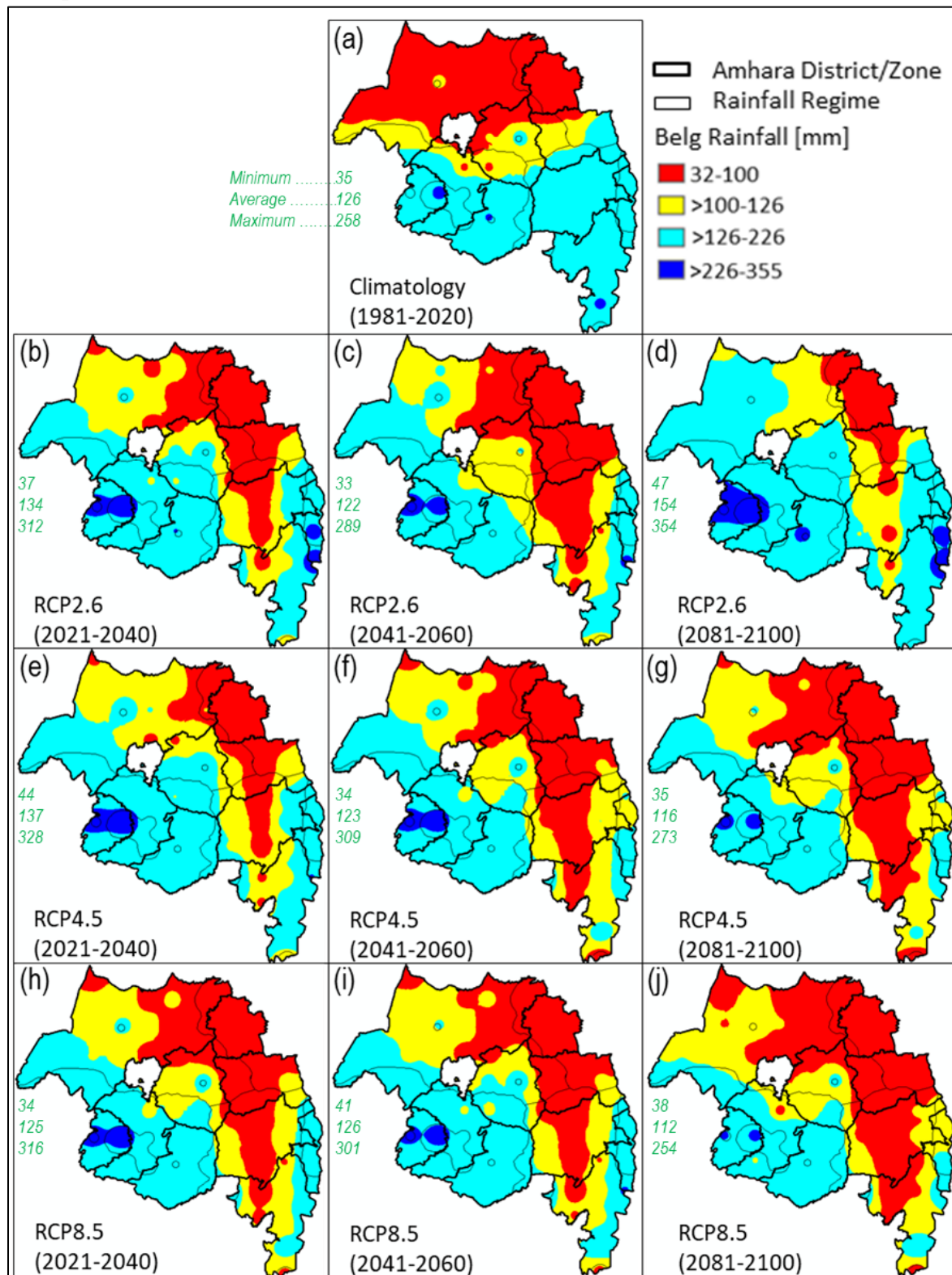
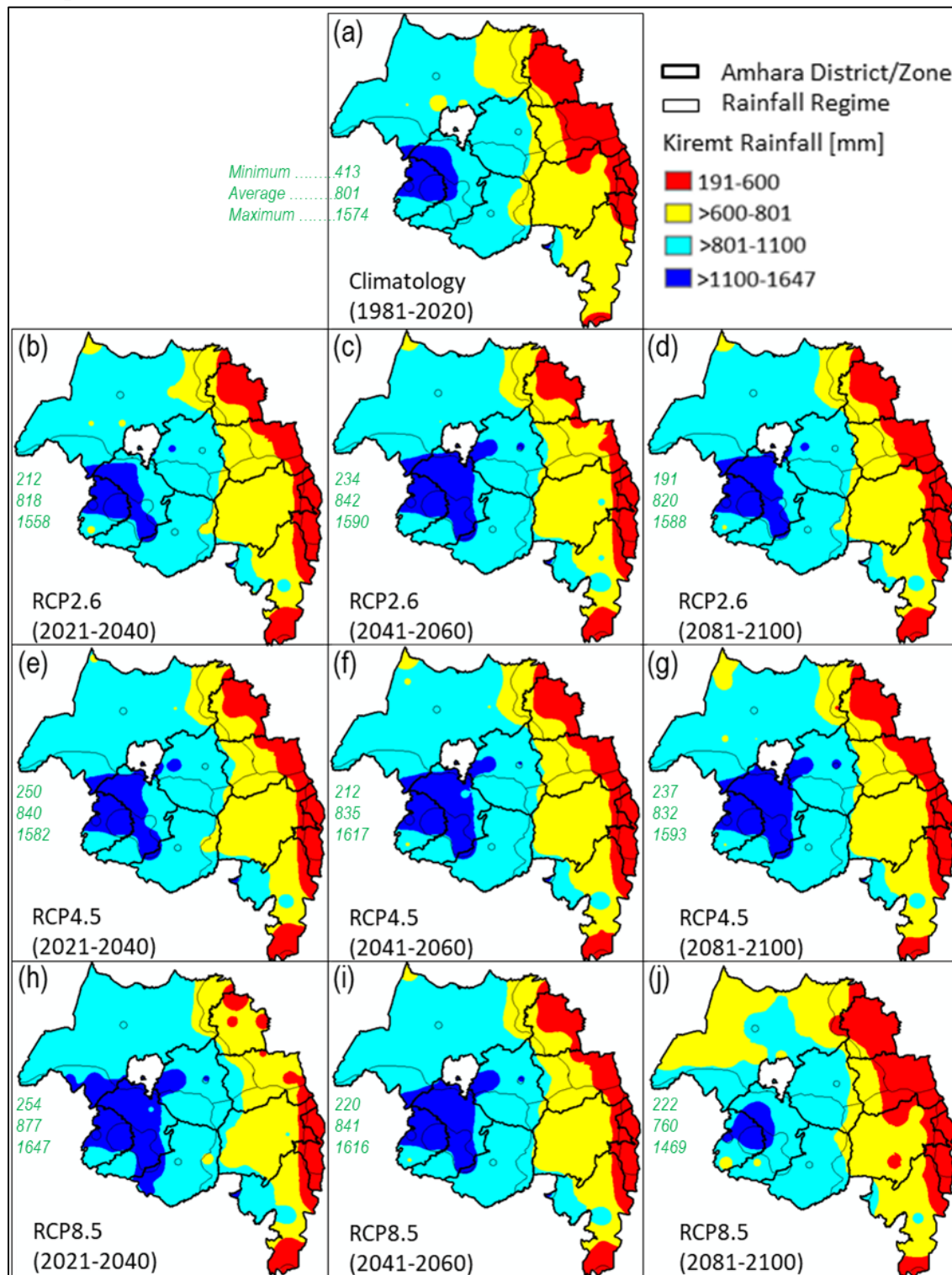


Figure 6: Historical (a) & future (b-j) Kiremt (Jun-Sep) average rainfall amount in Amhara, Ethiopia



DISCUSSIONS

Climatology

The mean rainfall of Amhara (ANRSE) based on 71 station and satellite merged data obtained from the Ethiopian Meteorology Institute (EMI) during

1981-2020 (40 years) was 990.2 mm, equivalent to 168 BCM (area of ANRSE = 170,000 km²).

Using the CHIRPS climate dataset of Amhara with a spatial resolution of 0.05° during 1981-2017, Alemu & Bawoke (2020) found the mean

annual total rainfall of Amhara to be 1,111 mm where July (284 mm) and August (287 mm) had the highest and December (9 mm) and January (11 mm) had the least monthly values. Their result agrees with ours, except that the CHIRPS rainfall amounts were slightly overestimated (see *Appendix 3*). According to (Bekele-Biratu et al. (2018), the climatology of northwest Ethiopia was around 1000 mm. Also, according to Mesfin et al. (2021), the mean annual rainfall of Amhara during 1987-2013 based on 23 observed and 119 CFSR reanalysis data was 1,150 mm, equivalent to 180 BCM (area of ANRSE = 157,134.5 km²).

Thus, the climatology result of our study is in alignment with the above studies. Generally, in climate science studies, particularly in climatology studies, using longer periods of at least 30 years is preferred to shorter periods. Also, observational data from meteorological offices is often more reliable than reanalysis data.

Historical Trend

As shown in *Table 1*, the trend analysis method used throughout this study (Eq. 2-6) was tested and validated using Mann-Kendal (MK) and

Innovative trend analysis (ITA) tests based on annual total rainfall amount data during 1981-2020 for Amhara and the five rainfall regimes of Amhara. The result showed that the correlation of the trends (slopes) between MK & Eq. 2, MK & ITA, and Eq. 2 & ITA methods was 0.93, 0.83, and 0.78, respectively; the correlation for the p-value between MK & Eq. 2 methods was 1.00. The test or validation result indicated that the trend analysis method used in this study was appropriate and accurate. Aligned with our study, Xu et al. (2021) also found similar results using a similar methodology (Eq. 2-6). Although ITA and the MK tests may result in similar trends, the ITA test outperforms the MK trend test because it does not have preconditions; the MK test has preconditions such as distribution type, size of dataset, and existence or non-existence of serial autocorrelation (Seenu & Jayakumar, 2021). Other studies conducted in Ethiopia reported that the ITA test can identify various significant trends not detected by the MK test (Likinaw et al., 2023) and was preferred to the MK test (Gedefaw, 2023). This study resulted in similar trend values for $f = 73$ and $f = 80.08$ with Eq. 2.

Table 1: Comparison of three trend methods for the annual rainfall amount in Amhara and its Regimes

| Trend Methods | Abbrev. | Trend indicators | Amhara | A3 | A4 | A5U | A5L | A6 | Avg |
|---------------------------------|------------|------------------|--------|------|------|------|------|------|------|
| Mann-Kendal Trend Test | MK | sen's slope | 2.13 | 1.50 | 0.29 | 2.78 | 1.57 | 2.18 | 1.74 |
| | | p-value | 0.03 | 0.13 | 0.77 | 0.01 | 0.12 | 0.03 | 0.18 |
| SLOPE function of MS Excel | Eq.2 | slope | 2.99 | 3.38 | 1.05 | 4.07 | 2.96 | 3.86 | 3.05 |
| | | p-value | 0.03 | 0.13 | 0.52 | 0.00 | 0.08 | 0.02 | 0.13 |
| Innovative Trend Analysis (ITA) | ITA | ϕ^a | 0.04 | 0.02 | 0.01 | 0.07 | 0.03 | 0.07 | 0.04 |
| | (ϕ) | ϕ^b | 2.70 | 1.25 | 0.76 | 4.76 | 2.34 | 4.89 | 2.78 |
| | | ϕ^c | 2.96 | 1.38 | 0.84 | 5.22 | 2.57 | 5.36 | 3.05 |

a, b, and c indicates ϕ values for multiplying factor (f) = 1, 73, and 80.08, respectively. Bold numbers indicate the trend is significant at 95% confidence level.

For the annual rainfall amount, the correlation of the trends (slopes) between MK & Eq. 2, MK & ITA, and Eq. 2 & ITA methods was 0.93, 0.83, and 0.78, respectively; the correlation for the p-value between MK & Eq. 2 methods was 1.00. Other scholars have also studied the rainfall trend in Amhara at different times and found different results. For example, Alemu & Bawoke (2020) found an overall annual and seasonal rainfall

increase (except winter or Dec-Feb) of Amhara during 1981-2017. Their result agrees with ours (see *Appendix 3*; particularly for Amhara case in Annual, Kiremt, Belg, and Dec-Feb).

In another study conducted in western Amhara from 1986 to 2015 in five districts (West Gojjam, East Gojjam, Awi, South Gonder, and North Gonder), each represented by three rainfall stations using Mann-Kendall trend analysis, four

districts showed a non-significant increasing annual rainfall trend; whereas, the rainfall in one district (West Gojjam) was decreasing (Amare et al., 2022). In another study conducted in the North Shoa district/Zone of Amhara from 1985 to 2018, Abegaz & Mekoya (2020) found increasing annual and Kiremt rainfall trends and decreasing Belg and Bega rainfall trends. Also, in another study conducted in east Amhara from 1985-2018, (Abera & Abegaz (2020) found increasing annual, Kiremt, Bega, and Belg rainfall trends over 65%, 85%, 70%, and 35% of the study areas, respectively.

In a previous study, the rainfall in Amhara did not show any decreasing or increasing trend from 1978 to 2008 (Ayalew et al., 2012b). In a recent study conducted at Upper Blue Nile Basin (UBNB) or “Abbay Basin,” which covers most of Amhara, using the CHIRPS-v2 dataset, the average annual rainfall increased (Ayehu et al., 2021) during 1981-2018. In another similar study conducted at UBNB using 26 stations data having missing days of <30%, Mohammed et al., 2022 reported increasing annual, March-May, and October-February rainfall and decreasing June-September rainfall in >54% and 65.4% of their study area, respectively. In another study conducted in the North Wollo district of Amhara, Bahiru & Zewdu (2021) found increasing annual and Kiremt and decreasing Belg rainfall during 1987-2017 using meteorological data from 17 stations.

In contrast to the above studies, in a survey conducted to know 168 farmers’ perceptions on rainfall trend in the Sekota district of Amhara region, 100% and 99.4% of the farmers answered uncertain for increasing trend and certain for decreasing trend, respectively (Behailu et al., 2021). Aligned with the farmers’ perception at Sekota, Mesfin et al. (2021) found a decreasing trend of annual rainfall in most (78.4%) areas of Amhara. In the Teff crop growing belts of Ethiopia, which includes all areas of Amhara, (Tirfi & Oyekale, 2022) found that short-season rainfall had a decreasing rainfall trend (-0.474 mm/year) with higher variability compared to the

long-season rainfall, which had an increasing trend (2.72 mm/year).

Future Projection

According to IPCC (AR6-WGI-Chapter 4), in the 21st century, an increase in annual global land precipitation has been projected with high confidence as globally averaged surface air temperature (GSAT) increases (Lee et al., 2021). All available CMIP6 models showed that relative to 1995-2014, the increase in precipitation during 2081-2100 will be more pronounced for high-emission scenario (SSP5-8.5) than for low-emission scenario (SSP1-1.9) (Lee et al., 2021). However, another study conducted in Ethiopia using CMIP5 model under RCP 4.5 and RCP 8.5 scenarios projected a decreasing rainfall in JJAS or Kiremt season and significant variability in FMAM or Belg season (Teshome & Zhang, 2019). The results of the above global and national studies partially agree with our regional study.

Uncertainties

Uncertainties may affect the result of this study. Uncertainties in rainfall projection may exist due to the selection of GCMs, RCMs, ensemble, model validation metrics, number of observation data used for testing and validating CORDEX GCMs, RCP scenarios of CMIP5, etc. For example, the result obtained for the patterns of the spatial distribution of the mean changes in the contribution of the wet days rainfall to the total seasonal rainfall and events of rainfall exceeding 10mm and 20mm in west Africa using CMIP6 projections (Worou et al., 2023) were different from the ones obtained using CMIP5 projections (Akinsanola & Zhou, 2019). Because, for a location, different datasets may differ in rainfall amount and pattern; also, the effect of orography may not be addressed in all model domains. For instance, Van Vooren et al. (2019) reported the high sensitivity of CORDEX ensemble means to orographic effect resulting in over- and under-estimations in the higher and lower study areas, respectively.

According to Van Vooren et al. (2019), the aspects of topography, such as elevation, slope,

geographical location, and slope orientation, shall be addressed. However, in this study, the different CORDEX domains and topography's effect were not considered independently while dealing with the rainfall trend and projection in the mountainous Amhara regional state of Ethiopia.

Rettie et al. (2023) found that the projected changes were dominated by GCM uncertainties and GCM and SSP uncertainties at the beginning and end of the projection period (21st century), respectively. Thus, the future rainfall trends of Amhara will not be free from the uncertainties mentioned by (Rettie et al., 2023).

Compared to the future period, uncertainties in historical rainfall trends of the Amhara regional state of Ethiopia will be negligibly small because the appropriate trend analysis method was used in this study, which also showed a high correlation with ITA and MK trend analysis methods that many scholars worldwide use. However, the region's rainfall trend is strongly affected by the choice of study period because of decadal variability, particularly from the 1980s (the driest decade) to the 1990s (the wettest decade) (Bewket & Conway, 2007).

Thus, ensuring reliable information production by the selected models and the existence of insignificant errors by uncertainties such as the ones listed above is a prerequisite before studying the impact of climate change in a complex climate region such as the mountainous Amhara regional state of Ethiopia.

SUMMARY, CONCLUSION AND RECOMMENDATION

Summary

A summary of future rainfall projections for the Amhara region indicates that annual and seasonal mean rainfall amounts are expected to be higher than historical averages. However, there are exceptions to this trend. In the near term, the Belg season shows a decrease in mean rainfall under RCP 8.5, and in the mid-term, both RCP 2.6 and RCP 4.5 show a decrease in Belg season rainfall. In the long-term, Belg season rainfall is projected

to decrease under RCP 4.5 and RCP 8.5. Additionally, long-term Kiremt and annual rainfall amounts under RCP 8.5 are expected to decrease compared to historical averages. Despite these changes, the future distribution pattern of mean rainfall amounts is expected to be similar to historical patterns, except for the Bega and Belg seasons, which will have distribution patterns different from historical records. Future mean rainfall amounts for the Bega and Belg seasons will have different magnitudes than historical averages, with values supported by their corresponding mean rainfall amounts. Specific rainfall amount ranges are provided for each period and season, indicating an increase in annual and Kiremt rainfall in the near- and mid-terms and a decrease in the long-term compared to historical averages. Bega rainfall is projected to increase in all future scenarios and periods, while Belg rainfall will experience unexpected changes.

Conclusion

The study provides valuable insights into the rainfall characteristics and spatial distribution in the Amhara National Regional State of Ethiopia. The region experiences a mean annual rainfall of 990.2 mm, peak amounts in August and July. Variations in rainfall distribution are observed, with the eastern-half receiving less rainfall than the western half. The study concludes that future rainfall patterns in the Amhara region are expected to change under different climate scenarios and periods. Overall, the projections suggest an increase in annual and seasonal mean rainfall amounts compared to historical averages. However, there are exceptions, such as a decrease in Belg season rainfall in certain scenarios and periods and a decrease in Kiremt and annual rainfall in the long term under specific scenarios. The future distribution pattern of mean rainfall amounts is anticipated to be similar to historical patterns, except for the Bega and Belg seasons, which will exhibit different distribution patterns. The magnitude of future rainfall amounts in Bega and Belg seasons will also differ from historical averages, supported by corresponding mean rainfall amounts. Overall, the results suggest that

Amhara's annual and Kiremt rainfall amounts are expected to increase in the near- and mid-terms compared to historical climatology. However, in the long-term, both the annual and Kiremt rainfall amounts are projected to decrease. On the other hand, Bega rainfall is projected to increase in all future terms and in all scenarios, while Belg rainfall will experience abrupt changes.

Recommendation:

Based on these findings, stakeholders in the Amhara region need to consider the projected changes in rainfall patterns for effective planning and decision-making. The following recommendations are suggested:

As rainfall patterns are expected to change, assessing and adapting water resource management strategies is crucial. This may involve developing storage facilities, improving irrigation systems, and promoting efficient water use practices to ensure sustainable water availability for agriculture, industry, and domestic use.

Farmers and agricultural policymakers should consider the projected changes in rainfall amounts and adjust cropping patterns, irrigation methods, and crop varieties accordingly. Diversifying crops and implementing climate-smart agricultural practices can help mitigate the potential impacts of changing rainfall patterns on agricultural productivity. Developing and implementing climate change adaptation strategies at the regional and local levels is essential. This may involve raising community awareness, providing access to climate information, promoting early warning systems, and supporting the adoption of climate-resilient practices in various sectors.

Monitoring rainfall patterns and their impacts is crucial for accurate forecasting and decision-making. Further research can focus on understanding the underlying causes of the projected changes, exploring additional adaptation measures, and assessing the socio-economic implications of altered rainfall patterns. By considering these recommendations, stakeholders can enhance their preparedness and

resilience to the expected changes in rainfall patterns, thereby minimizing potential risks and maximizing opportunities for sustainable development in the Amhara region.

ACKNOWLEDGMENTS

The authors thank the Ethiopia Meteorology Institute (EMI), also called the National Meteorology Agency of Ethiopia, and the CORDEX project for providing or allowing access to long years of climate data. The authors also thank Dr. Adefires Worku, Dr. Zenebe Mekonnen, and Dr. Abeje Eshete for creating or supervising a mega project in which this activity is a part and Mr. Alem Getachew for sharing valuable climate modeling experience. The authors are also grateful for the valuable contribution received from Mr. Abebe Guadie. Moreover, the authors also thank the Ethiopian Forestry Development, which was previously called the Ethiopia Environment and Forest Research Institute, and the anonymous reviewers.

Conflict Of Interest

The authors declare that they have no conflict of interest.

Declarations

Data Availability Statement

The dataset used in this study can be found from third parties such as Ethiopia Meteorology Institute formerly called the National Meteorology Agency of Ethiopia (<http://www.ethiomet.gov.et/>) and other climate dataset website URLs listed in the main manuscript document.

REFERENCES

- Abegaz, W. B., & Mekoya, A. (2020). Rainfall Variability and Trends over Central Ethiopia. *International Journal of Environmental Sciences & Natural Resources*, 24(4). <https://doi.org/10.19080/ijesnr.2020.24.556144>
- Abera, E. A., & Abegaz, W. B. (2020). *Climatology & Weather Forecasting Seasonal*

- and Annual Rainfall Trend Detection in Eastern Amhara, *Journal of Climatology & Weather Forecasting*, 1–10. <https://doi.org/10.35248/2332-2594.2020.8.264>
- Akinsanola, A. A., & Zhou, W. (2019). Projections of West African summer monsoon rainfall extremes from two CORDEX models. *Climate Dynamics*, 52(3–4), 2017–2028. <https://doi.org/10.1007/s00382-018-4238-8>
- Alemu, M. M., & Bawoke, G. T. (2020). Analysis of spatial variability and temporal trends of rainfall in Amhara Region, Ethiopia. *Journal of Water and Climate Change*, 11(4), 1505–1520. <https://doi.org/10.2166/wcc.2019.084>
- Amare, Z., Geremew, B., Kebede, N., & Amara, S. (2022). Climate Trends, variability, and impacts of ENSO on rainfall amount in Ethiopia: A Case study in Western Amhara National Regional State. *Research Square*, 1–20. <https://doi.org/https://doi.org/10.21203/rs.3.rs-2078316/v1>
- Ayalew, D., Tesfaye, K., Mamo, G., Yitaferu, B., & Bayu, W. (2012a). Outlook of future climate in northwestern Ethiopia. *Agricultural Sciences*, 03(04), 608–624. <https://doi.org/10.4236/as.2012.34074>
- Ayalew, D., Tesfaye, K., Mamo, G., Yitaferu, B., & Bayu, W. (2012b). Variability of rainfall and its current trend in Amhara region, Ethiopia. *African Journal of Agricultural Research*, 7(10), 1475–1486. <https://doi.org/10.5897/AJAR11.698>
- Ayehu, G. T., Tadesse, T., & Gessesse, B. (2021). Spatial and temporal trends and variability of rainfall using long-term satellite product over the Upper Blue Nile Basin in Ethiopia. *Remote Sensing in Earth Systems Sciences*, 4(3), 199–215. <https://doi.org/10.1007/s41976-021-00060-3>
- Azadi, H., Moghaddam, S. M., Mahmoudi, H., Burkart, S., Debela, D. D., Teklemariam, D., & Lodin, M. (2020). *Impacts of the Land Tenure System on Sustainable Land Use in Ethiopia*. December 2018, 225–261.
- Bahiru, W., & Zewdu, E. (2021). Analysis of Spatial and Temporal Climate Characteristics in North Eastern Ethiopia: Case Study of North Wollo Zone. *International Journal of Energy and Environmental Science*, 6(3), 57. <https://doi.org/10.11648/j.ijees.20210603.12>
- Behailu, G., Yayeh, D., Terefe, T., & Ture, K. (2021). Comparative Analysis of Meteorological Records of Climate Variability and Farmers' Perceptions in Sekota Woreda, Ethiopia. *Climate Services*, 23, 100239. <https://doi.org/10.1016/j.cliser.2021.100239>
- Bekele-Biratu, E., Thiaw, W. M., & Korecha, D. (2018). Sub-seasonal variability of the Belg rains in Ethiopia. *International Journal of Climatology*, 38(7), 2940–2953. <https://doi.org/10.1002/joc.5474>
- Belay, A. S., Fenta, A. A., Yenahun, A., Nigate, F., Tilahun, S. A., Moges, M. M., Dessie, M., Adgo, E., Nyssen, J., Chen, M., Griensven, A. Van, & Walraevens, K. (2019). *Evaluation and Application of Multi-Source Satellite Rainfall Product CHIRPS to Assess Spatio-Temporal Rainfall Variability on Data-Sparse Western Margins of Ethiopian Highlands*. 1–22.
- Berhane, A., Hadgu, G., Worku, W., & Abrha, B. (2020). Trends in extreme temperature and rainfall indices in the semi-arid areas of Western Tigray, Ethiopia. *Environmental Systems Research*, 9(1). <https://doi.org/10.1186/s40068-020-00165-6>
- Bewket, W., & Conway, D. (2007). *A note on the temporal and spatial variability of rainfall in the drought-prone Amhara region of Ethiopia*. 1477(May), 1467–1477. <https://doi.org/10.1002/joc.1481>
- Birara, H., Pandey, R. P., & Mishra, S. K. (2018). Trend and variability analysis of rainfall and temperature in the tana basin region, Ethiopia. *Journal of Water and Climate Change*, 9(3),

- 555–569.
<https://doi.org/10.2166/wcc.2018.080>
- Braun, J. Von. (1991). A Policy Agenda for Famine. Prevention in Africa. *International Food Policy Institute*, 13, 2.
<https://www.ifpri.org/publication/policy-agenda-famine-prevention-africa>
- Cochrane, L., & Vercillo, S. (2019). Youth perspectives:: migration, poverty, and the future of farming in rural Ethiopia. *Bristol: Polity Press*, 277–96.
- CSA. (2007). *The 2007 Population and Housing Census of Ethiopia: Federal Democratic Republic of Ethiopia Population Census Commission*. 1–125.
- Demaeyer, J., Penny, S. G., & Vannitsem, S. (2022). Identifying Efficient Ensemble Perturbations for Initializing Subseasonal-To-Seasonal Prediction. *Journal of Advances in Modeling Earth Systems*, 14(5).
<https://doi.org/10.1029/2021MS002828>
- FAO. (2014). *Food and Agriculture Organization of the United Nations Regional Office for Africa*. FAO. <https://doi.org/https://www.fao.org/3/i3620e/i3620e.pdf>
- Gebrechorkos, S. H., Hülsmann, S., & Bernhofer, C. (2019). Changes in temperature and precipitation extremes in Ethiopia, Kenya, and Tanzania. *International Journal of Climatology*, 39(1), 18–30.
<https://doi.org/10.1002/joc.5777>
- Gedefaw, M. (2023). Assessment of changes in climate extremes of temperature over Ethiopia. *Cogent Engineering*, 10(1).
<https://doi.org/10.1080/23311916.2023.2178117>
- Grose, M. R., Narsey, S., Trancoso, R., Mackallah, C., Delage, F., Dowdy, A., Di Virgilio, G., Watterson, I., Dobrohotoff, P., Rashid, H. A., Rauniyar, S., Henley, B., Thatcher, M., Syktus, J., Abramowitz, G., Evans, J. P., Su, C. H., & Takbash, A. (2023). A CMIP6-based multi-model downscaling ensemble to underpin climate change services in Australia. *Climate Services*, 30(August 2022). <https://doi.org/10.1016/j.cliser.2023.100368>
- Haile, M., Herweg, K., & Stillhardt, B. (2006). *Sustainable Land Management – A New Approach to Soil and Water Conservation in Ethiopia Sustainable Land Management – A New Approach to Soil and Water Conservation in Ethiopia*.
- Harris, I., Osborn, T. J., Jones, P., & Lister, D. (2020). Version 4 of the CRU TS monthly high-resolution gridded multivariate climate dataset. *Scientific Data*, 7(1), 1–19.
<https://doi.org/10.1038/s41597-020-0453-3>
- Herger, N., Abramowitz, G., Knutti, R., Angélil, O., Lehmann, K., & Sanderson, B. M. (2018). Selecting a climate model subset to optimise key ensemble properties. *Earth System Dynamics*, 9(1), 135–151.
<https://doi.org/10.5194/esd-9-135-2018>
- Huang, Z. P., & Chen, Y. F. (2011). *Hydrostatistics (in Chinese)*. Beijing, China: China Waterpower Press, 1st edition., 209e.
- IPCC. (2019). Climate Change and Land: an IPCC special report. *Climate Change and Land: An IPCC Special Report on Climate Change, Desertification, Land Degradation, Sustainable Land Management, Food Security, and Greenhouse Gas Fluxes in Terrestrial Ecosystems*, 1–864.
<https://www.ipcc.ch/srccl/>
- Jabal, Z. K., Khayyun, T. S., & Alwan, I. A. (2022). *Impact of Climate Change on Crops Productivity Using MODIS-NDVI Time Series*. June. <https://doi.org/10.28991/CEJ-2022-08-06-04>
- Jain, S. K., Kumar, V., & Saharia, M. (2013). Analysis of rainfall and temperature trends in northeast India. *International Journal of Climatology Published by John Wiley & Sons Ltd on Behalf of Royal Meteorological Society*, 978(April 2012), 968–978.
<https://doi.org/10.1002/joc.3483>

- Kamalanandhini, M., & Annadurai, R. (2021). Assessment of five meteorological indices for monitoring the drought condition in Chengalpattu District, Tamilnadu, India. *Materials Today: Proceedings*, 46(xxxx), 3699–3703. <https://doi.org/10.1016/j.matpr.2021.01.850>
- Kassahun, M., Ture, K., & Nedaw, D. (2023). Evaluation of CORDEX Africa regional climate models performance in simulating climatology of Zarima sub - basin northwestern Ethiopia. *Environmental Systems Research*. <https://doi.org/10.1186/s40068-023-00325-4>
- Lee, J.-Y., Marotzke, J., Bala, G., Cao, L., Corti, S., Dunne, J., Engelbrecht, F., Fischer, E., Fyfe, J., Jones, C., Maycock, A., Mutemi, J., Ndiaye, O., Panickal, S., & Zhou, T. (2021). Future global climate: scenario-based projections and near-term information. In *Climate Change 2021: The Physical Science Basis. Contribution of Working Group I to the Sixth Assessment Report of the Intergovernmental Panel on Climate Change*. <https://doi.org/10.1017/9781009157896.006.553>
- Likinaw, A., Alemayehu, A., & Bewket, W. (2023). Trends in Extreme Precipitation Indices in Northwest Ethiopia: Comparative Analysis Using the Mann–Kendall and Innovative Trend Analysis Methods. *Climate*, 11(8). <https://doi.org/10.3390/cli11080164>
- Luhunga, P. M., Kijazi, A. L., Chang’a, L., Kondowe, A., Ng’ongolo, H., & Mtongori, H. (2018). Climate change projections for Tanzania Based on high-resolution regional climate models from the Coordinated Regional Climate Downscaling Experiment (CORDEX)-Africa. *Frontiers in Environmental Science*, 6(OCT), 1–20. <https://doi.org/10.3389/fenvs.2018.00122>
- Mekoya, A., & Molla, M. (2024). Testing CORDEX GCMs for Projecting Rainfall in Amhara, Ethiopia. *African Journal of Climate Change and Resource Sustainability*, 3(1), 24–48. <https://doi.org/10.37284/ajccrs.3.1.1730.24>
- Mesfin, S., Adem, A. A., Mullu, A., & Melesse, A. M. (2021). Historical Trend Analysis of Rainfall in Amhara National Regional State (Chapter 25 of a book: Nile and Grand Ethiopian Renaissance Dam, Springer Geography). *Springer Nature Switzerland AG 2021 A. M. Melesse et Al. (Eds.), September*. <https://doi.org/10.1007/978-3-030-76437-1>
- Musayev, S., Mellor, J., Walsh, T., & Anagnostou, E. (2021). Development of an agent-based model for weather forecast information exchange in rural area of bahir dar, ethiopia. *Sustainability (Switzerland)*, 13(9). <https://doi.org/10.3390/su13094936>
- NMA. (1996). Climatic and Agroclimatic Resources of Ethiopia. *Climatic and Agroclimatic Resources of Ethiopia*.
- Rettie, F. M., Gayler, S., Weber, T. K. D., Tesfaye, K., & Streck, T. (2023). Comprehensive assessment of climate extremes in high-resolution CMIP6 projections for Ethiopia. *Frontiers in Environmental Science*, 11(May). <https://doi.org/10.3389/fenvs.2023.1127265>
- Salas, J. D. (1993). Analysis and Modeling of Hydrological Time Series. *Handbook of Hydrology*, McGraw-Hill, New York, 19.1-19.72.
- Seenu, P. Z., & Jayakumar, K. V. (2021). Comparative study of innovative trend analysis technique with Mann-Kendall tests for extreme rainfall. *Arabian Journal of Geosciences*, 14(7). <https://doi.org/10.1007/s12517-021-06906-w>
- Seleshi, Y., & Zanke, U. (2004). Recent changes in rainfall and rainy days in Ethiopia. *International Journal of Climatology*, 24(8), 973–983. <https://doi.org/10.1002/joc.1052>
- Şen, Z. (2012). Innovative Trend Analysis Methodology. *Journal of Hydrologic Engineering*, 17(9). [https://doi.org/10.1061/\(ASCE\)HE.1943-5584.0000556](https://doi.org/10.1061/(ASCE)HE.1943-5584.0000556)

- Sisay, K., Thurnher, C., & Hasenauer, H. (2017). Daily climate data for the Amhara region in Northwestern Ethiopia. *International Journal of Climatology*, 37(6), 2797–2808. <https://doi.org/10.1002/joc.4880>
- Sisay, K., Vienna, L. S., Thurnher, C., Vienna, L. S., Hasenauer, H., & Vienna, L. S. (2016). Daily climate data for the Amhara region in Northwestern. *INTERNATIONAL JOURNAL OF CLIMATOLOGY*. <https://doi.org/10.1002/joc.4880>
- SUN, S., CHEN, H., SUN, G., JU, W., WANG, G., LI, X., YAN, G., GAO, C., HUANG, J., ZHANG, F., ZHU, S., & HUA, W. (2017). Attributing the Changes in Reference Evapotranspiration in Southwestern China Using a New Separation Method. *American Meteorological Society*, 777–798. <https://doi.org/10.1175/JHM-D-16-0118.1>
- Terefe, S., Bantider, A., Teferi, E., & Abi, M. (2022). Spatiotemporal trends in mean and extreme climate variables over 1981–2020 in Meki watershed of central rift valley basin, Ethiopia. *Heliyon*, 8(11), e11684. <https://doi.org/10.1016/j.heliyon.2022.e11684>
- Teshome, A., & Zhang, J. (2019). Increase of extreme drought over Ethiopia under climate warming. *Advances in Meteorology*, 2019. <https://doi.org/10.1155/2019/5235429>
- Tirfi, A. G., & Oyekale, A. S. (2022). Analysis of trends and variability of climatic parameters in Teff growing belts of Ethiopia. *Open Agriculture*, 7(1), 541–553. <https://doi.org/10.1515/opag-2022-0113>
- UNICEF. (2018). Budget Brief Amhara Regional State 2007/08 – 2015/16. *Unicef*, 1–16.
- Van Vooren, S., Van Schaeybroeck, B., Nyssen, J., Van Ginderachter, M., & Termonia, P. (2019). Evaluation of CORDEX rainfall in northwest Ethiopia: Sensitivity to the model representation of the orography. *International Journal of Climatology*, 39(5), 2569–2586. <https://doi.org/10.1002/joc.5971>
- Ware, M. B., Matewos, T., Guye, M., Legesse, A., & Mohammed, Y. (2023). Spatiotemporal variability and trend of rainfall and temperature in Sidama Regional State, Ethiopia. *Theoretical and Applied Climatology*, 153(1–2), 213–226. <https://doi.org/10.1007/s00704-023-04463-8>
- Worou, K., Fichet, T., & Goosse, H. (2023). Future changes in the mean and variability of extreme rainfall indices over the Guinea coast and role of the Atlantic equatorial mode. *Weather and Climate Dynamics*, 4(2), 511–530. <https://doi.org/10.5194/wcd-4-511-2023>
- Wubaye, G. B., Gashaw, T., Worqlul, A. W., Dile, Y. T., Taye, M. T., Haileslassie, A., Zaitchik, B., Birhan, D. A., Adgo, E., Mohammed, J. A., Lebeza, T. M., Bantider, A., Seid, A., & Srinivasan, R. (2023). Trends in Rainfall and Temperature Extremes in Ethiopia: Station and Agro-Ecological Zone Levels of Analysis. *Atmosphere*, 14(3). <https://doi.org/10.3390/atmos14030483>
- Xu, L., Sun, S., Chen, H., Chai, R., Wang, J., Zhou, Y., Ma, Q., Chotamonsak, C., & Wangpakapattanawong, P. (2021). Changes in the reference evapotranspiration and contributions of climate factors over the Indo – China Peninsula during 1961 – 2017. *International Journal of Climatology Published by John Wiley & Sons Ltd on Behalf of Royal Meteorological Society.*, December 2020, 1–19. <https://doi.org/10.1002/joc.7209>
- Yimer, S. M., Bouanani, A., Kumar, N., Tischbein, B., & Borgemeister, C. (2022). Assessment of Climate Models Performance and Associated Uncertainties in Rainfall Projection from CORDEX over the Eastern Nile Basin, Ethiopia. *Climate*, 10(7). <https://doi.org/10.3390/cli10070095>
- Zegeye, M. K., Bekitie, K. T., & Hailu, D. N. (2022). Spatio - temporal variability and trends of hydroclimatic variables at Zarima Sub - Basin North Western Ethiopia. *Environmental Systems Research*, 5. <https://doi.org/10.1186/s40068-022-00273-5>

APPENDICES

Appendix 1: Trend/slope (b), p-value, and Intercept (a) of rainfall for linear regression analysis: $y = a + bx$ where y is rainfall amount and x is time (1-39 for the years 1981-2020) in Amhara and its five Rainfall Regimes (A3-A6)

| Place | Parameter | Annual | Bega | Belg | Kiremt | Jan | Feb | Mar | Apr | May | Jun | Jul | Aug | Sep | Oct | Nov | Dec |
|--------|---------------|--------|-------|-------|--------|-------|-------|-------|-------|------|-------|-------|------|-------|-------|------|-------|
| Amhara | slope (b) | 2.99 | 0.25 | 0.33 | 2.42 | -0.12 | -0.08 | -0.23 | 0.04 | 0.59 | 0.39 | 0.70 | 1.09 | 0.23 | 0.02 | 0.39 | -0.04 |
| | p-value | 0.03 | 0.64 | 0.61 | 0.05 | 0.05 | 0.41 | 0.29 | 0.86 | 0.21 | 0.29 | 0.30 | 0.01 | 0.52 | 0.96 | 0.02 | 0.63 |
| | intercept (a) | 929 | 58 | 119 | 751 | 7 | 8 | 27 | 32 | 52 | 108 | 262 | 257 | 125 | 43 | 3 | 5 |
| A3 | slope (b) | 3.38 | 0.79 | 1.80 | 0.79 | -0.22 | 0.07 | 0.05 | 0.30 | 1.38 | 0.54 | -0.64 | 0.14 | 0.75 | 0.25 | 0.58 | 0.19 |
| | p-value | 0.14 | 0.43 | 0.09 | 0.60 | 0.11 | 0.52 | 0.87 | 0.50 | 0.10 | 0.32 | 0.33 | 0.84 | 0.15 | 0.75 | 0.04 | 0.33 |
| | intercept (a) | 1445 | 129 | 165 | 1151 | 10 | 5 | 25 | 35 | 99 | 214 | 366 | 350 | 221 | 99 | 13 | 7 |
| A4 | slope (b) | 1.05 | 0.46 | 1.02 | -0.43 | -0.06 | 0.07 | -0.05 | 0.11 | 0.88 | -0.19 | -0.47 | 0.06 | 0.18 | -0.02 | 0.52 | 0.02 |
| | p-value | 0.52 | 0.46 | 0.19 | 0.77 | 0.12 | 0.28 | 0.79 | 0.70 | 0.16 | 0.69 | 0.52 | 0.91 | 0.68 | 0.97 | 0.01 | 0.73 |
| | intercept (a) | 1180 | 78 | 114 | 987 | 3 | 1 | 15 | 25 | 73 | 181 | 330 | 304 | 173 | 70 | 3 | 3 |
| A5U | slope (b) | 4.07 | 0.34 | 0.94 | 2.79 | -0.01 | 0.04 | 0.01 | 0.11 | 0.78 | 0.47 | 0.75 | 1.07 | 0.50 | 0.02 | 0.29 | 0.04 |
| | p-value | 0.00 | 0.50 | 0.12 | 0.03 | 0.68 | 0.24 | 0.91 | 0.51 | 0.11 | 0.31 | 0.22 | 0.01 | 0.22 | 0.96 | 0.02 | 0.25 |
| | intercept (a) | 912 | 43 | 66 | 803 | 1 | 0 | 6 | 13 | 47 | 139 | 266 | 265 | 133 | 41 | 0 | 0 |
| A5L | slope (b) | 2.96 | -0.05 | -1.06 | 4.07 | -0.23 | -0.37 | -0.59 | -0.16 | 0.06 | 0.70 | 1.68 | 1.76 | -0.07 | -0.05 | 0.35 | -0.12 |
| | p-value | 0.09 | 0.93 | 0.23 | 0.01 | 0.08 | 0.05 | 0.19 | 0.73 | 0.91 | 0.11 | 0.11 | 0.01 | 0.86 | 0.88 | 0.13 | 0.42 |
| | intercept (a) | 820 | 52 | 179 | 589 | 14 | 22 | 56 | 57 | 44 | 35 | 231 | 235 | 89 | 24 | 5 | 9 |
| A6 | slope (b) | 3.86 | 0.00 | -0.19 | 4.05 | -0.20 | -0.12 | -0.45 | 0.03 | 0.35 | 0.56 | 1.42 | 1.99 | 0.09 | 0.08 | 0.34 | -0.22 |
| | p-value | 0.02 | 1.00 | 0.81 | 0.01 | 0.06 | 0.45 | 0.15 | 0.92 | 0.37 | 0.06 | 0.11 | 0.01 | 0.79 | 0.74 | 0.08 | 0.06 |
| | intercept (a) | 570 | 37 | 106 | 426 | 11 | 11 | 36 | 34 | 25 | 22 | 169 | 176 | 60 | 12 | 3 | 11 |

Appendix 2: Annual, Oct-Jan, Feb-May, and Jun-Sep number of significantly increasing (SI), Non-significantly Increasing (NI), Non-significantly Decreasing (ND), and Significantly Decreasing (SD) grid points in Amhara and its five Rainfall Regimes (A3-A6) during 19

| Time | Place | SI | NI | ND | SD | Place | SI | NI | ND | SD |
|--------|--------|----|----|----|----|-------|----|----|----|----|
| Annual | Amhara | 31 | 25 | 11 | 4 | A5U | 8 | 6 | 4 | 1 |
| Bega | | 4 | 57 | 10 | 0 | | 1 | 15 | 3 | 0 |
| Belg | | 14 | 33 | 22 | 2 | | 7 | 7 | 5 | 0 |
| Kiremt | | 28 | 22 | 16 | 5 | | 6 | 7 | 5 | 1 |
| Annual | A3 | 1 | 3 | 1 | 0 | A5L | 9 | 6 | 1 | 1 |
| Bega | | 1 | 4 | 0 | 0 | | 0 | 14 | 3 | 0 |
| Belg | | 1 | 4 | 0 | 0 | | 0 | 8 | 7 | 2 |
| Kiremt | | 1 | 1 | 3 | 0 | | 9 | 6 | 1 | 1 |
| Annual | A4 | 7 | 4 | 4 | 2 | A6 | 6 | 6 | 1 | 0 |
| Bega | | 1 | 16 | 0 | 0 | | 1 | 8 | 4 | 0 |
| Belg | | 3 | 10 | 4 | 0 | | 3 | 4 | 6 | 0 |
| Kiremt | | 4 | 5 | 5 | 3 | | 8 | 3 | 2 | 0 |

Appendix 3: Mean monthly, seasonal, and annual rainfall amount (Climatology) in mm in Amhara and its five rainfall regimes (A3-A6) during 1981-2020

| Time | Amhara | A3 | A4 | A5U | A5L | A6 | Time | Amhara | A3 | A4 | A5U | A5L | A6 |
|------|--------|-------|-------|-------|-------|-------|--------|--------|-------|-------|-------|-------|-------|
| Jan | 4.4 | 5.5 | 1.6 | 0.7 | 9 | 7 | Sep | 129.5 | 236.7 | 177.2 | 143 | 87.4 | 61.4 |
| Feb | 6.5 | 6.9 | 2.8 | 1.2 | 14 | 9.1 | Oct | 43 | 103.8 | 69.2 | 41.8 | 22.8 | 13.5 |
| Mar | 22.2 | 26 | 13.7 | 6.5 | 43.7 | 26.9 | Nov | 11.4 | 25.2 | 13.8 | 6.1 | 11.9 | 10.1 |
| Apr | 32.7 | 41.4 | 27.3 | 14.8 | 54.3 | 34.1 | Dec | 4.7 | 10.6 | 3.3 | 1.3 | 7 | 6.1 |
| May | 64.4 | 127.5 | 90.8 | 63.2 | 45.1 | 32.4 | Bega | 63.5 | 145.1 | 87.9 | 49.8 | 50.7 | 36.8 |
| Jun | 115.8 | 225.4 | 176.6 | 148.6 | 49.3 | 33.1 | Belg | 125.8 | 201.8 | 134.6 | 85.6 | 157.2 | 102.6 |
| Jul | 276.4 | 352.9 | 320.1 | 281 | 265.5 | 197.6 | Kiremt | 801 | 1167 | 978.7 | 859.7 | 672.8 | 509.3 |
| Aug | 279.2 | 352.4 | 304.7 | 287.2 | 270.7 | 217.2 | Annual | 990.2 | 1514 | 1201 | 995.2 | 880.6 | 648.7 |

Appendix 4: Trend/slope (b), p-value, and Intercept (a) of rainfall for linear regression analysis: $y = a + bx$ where y is rainfall amount and x is time (2021-2100) in Amhara and its five Rainfall Regimes (A3-A6) for RCP 2.6 Scenario

| Place | Parameter | Annual | Bega | Belg | Kiremt | Jan | Feb | Mar | Apr | May | Jun | Jul | Aug | Sep | Oct | Nov | Dec |
|--------|---------------|--------|-------|-------|--------|------|-------|-------|------|-------|-------|------|-------|-------|-------|-------|-------|
| Amhara | slope (b) | -0.20 | -0.18 | -0.20 | -0.25 | 0.02 | -0.02 | 0.08 | 0.16 | 0.01 | -0.17 | 0.22 | -0.08 | -0.21 | -0.16 | -0.08 | 0.04 |
| | p-value | 0.65 | 0.32 | 0.65 | 0.48 | 0.56 | 0.65 | 0.22 | 0.20 | 0.96 | 0.15 | 0.22 | 0.60 | 0.20 | 0.27 | 0.32 | 0.50 |
| | intercept (a) | 1441 | 447 | 1441 | 1327 | -34 | 44 | -141 | -280 | 43 | 449 | -202 | 474 | 606 | 360 | 188 | -66 |
| A3 | slope (b) | -0.19 | -0.49 | -0.19 | 0.01 | 0.02 | 0.03 | 0.05 | 0.17 | 0.03 | -0.20 | 0.31 | -0.07 | -0.04 | -0.21 | -0.14 | -0.16 |
| | p-value | 0.75 | 0.08 | 0.75 | 0.99 | 0.69 | 0.66 | 0.66 | 0.39 | 0.87 | 0.16 | 0.16 | 0.78 | 0.79 | 0.32 | 0.28 | 0.09 |
| | intercept (a) | 1977 | 1130 | 1977 | 1207 | -36 | -58 | -68 | -269 | 34 | 630 | -265 | 524 | 318 | 512 | 309 | 345 |
| A4 | slope (b) | -0.02 | -0.25 | -0.02 | 0.00 | 0.02 | 0.00 | 0.07 | 0.13 | 0.03 | -0.18 | 0.32 | -0.04 | -0.11 | -0.16 | -0.07 | -0.04 |
| | p-value | 0.97 | 0.19 | 0.97 | 0.99 | 0.50 | 0.97 | 0.31 | 0.29 | 0.85 | 0.20 | 0.05 | 0.81 | 0.54 | 0.31 | 0.36 | 0.41 |
| | intercept (a) | 1276 | 589 | 1276 | 1005 | -36 | 5 | -117 | -224 | 18 | 524 | -370 | 418 | 433 | 370 | 160 | 96 |
| A5U | slope (b) | 0.10 | -0.18 | 0.10 | 0.03 | 0.01 | 0.00 | -0.01 | 0.16 | 0.10 | -0.13 | 0.30 | 0.04 | -0.19 | -0.13 | -0.06 | 0.01 |
| | p-value | 0.80 | 0.16 | 0.80 | 0.94 | 0.48 | 0.87 | 0.87 | 0.13 | 0.47 | 0.38 | 0.06 | 0.81 | 0.32 | 0.25 | 0.12 | 0.87 |
| | intercept (a) | 836 | 401 | 836 | 836 | -24 | 11 | 27 | -292 | -147 | 390 | -371 | 251 | 566 | 290 | 139 | -5 |
| A5L | slope (b) | -0.52 | -0.11 | -0.52 | -0.62 | 0.01 | -0.04 | 0.17 | 0.15 | -0.08 | -0.19 | 0.03 | -0.18 | -0.28 | -0.16 | -0.06 | 0.10 |
| | p-value | 0.34 | 0.62 | 0.34 | 0.15 | 0.82 | 0.40 | 0.06 | 0.28 | 0.58 | 0.05 | 0.91 | 0.39 | 0.16 | 0.30 | 0.60 | 0.14 |
| | intercept (a) | 1990 | 311 | 1990 | 1978 | -8 | 100 | -338 | -267 | 207 | 448 | 170 | 657 | 703 | 371 | 143 | -195 |
| A6 | slope (b) | -0.45 | -0.07 | -0.45 | -0.57 | 0.05 | -0.05 | 0.10 | 0.19 | -0.05 | -0.16 | 0.17 | -0.20 | -0.38 | -0.17 | -0.14 | 0.19 |
| | p-value | 0.37 | 0.79 | 0.37 | 0.12 | 0.56 | 0.43 | 0.20 | 0.18 | 0.69 | 0.05 | 0.42 | 0.36 | 0.02 | 0.30 | 0.28 | 0.11 |
| | intercept (a) | 1616 | 245 | 1616 | 1661 | -81 | 109 | -187 | -357 | 144 | 369 | -199 | 614 | 878 | 375 | 307 | -355 |

Appendix 5: Trend/slope (b), p-value, and Intercept (a) of rainfall for linear regression analysis: $y = a + bx$ where y is rainfall amount and x is time (2021-2100) in Amhara and its five Rainfall Regimes (A3-A6) for RCP 4.5 Scenario

| Place | Parameter | Annual | Bega | Belg | Kiremt | Jan | Feb | Mar | Apr | May | Jun | Jul | Aug | Sep | Oct | Nov | Dec |
|--------|---------------|--------|------|-------|--------|------|-------|-------|-------|-------|-------|-------|------|-------|------|-------|-------|
| Amhara | slope (b) | -0.55 | 0.09 | -0.55 | -0.28 | 0.05 | -0.03 | 0.03 | -0.20 | -0.16 | -0.28 | -0.28 | 0.33 | -0.05 | 0.04 | 0.06 | -0.06 |
| | p-value | 0.22 | 0.65 | 0.22 | 0.46 | 0.18 | 0.39 | 0.66 | 0.07 | 0.23 | 0.01 | 0.13 | 0.02 | 0.76 | 0.72 | 0.60 | 0.33 |
| | intercept (a) | 2173 | -110 | 2173 | 1410 | -103 | 69 | -39 | 454 | 390 | 687 | 813 | -374 | 284 | -46 | -93 | 132 |
| A3 | slope (b) | -0.89 | 0.01 | -0.89 | -0.25 | 0.04 | -0.08 | -0.06 | -0.33 | -0.16 | -0.35 | -0.33 | 0.43 | -0.01 | 0.11 | -0.04 | -0.10 |
| | p-value | 0.12 | 0.98 | 0.12 | 0.57 | 0.45 | 0.26 | 0.61 | 0.06 | 0.40 | 0.02 | 0.17 | 0.04 | 0.94 | 0.57 | 0.77 | 0.26 |
| | intercept (a) | 3407 | 118 | 3407 | 1753 | -75 | 187 | 164 | 756 | 429 | 933 | 1053 | -500 | 268 | -165 | 124 | 235 |
| A4 | slope (b) | -0.49 | 0.05 | -0.49 | -0.19 | 0.03 | -0.04 | 0.00 | -0.21 | -0.11 | -0.38 | -0.22 | 0.39 | 0.02 | 0.04 | 0.04 | -0.06 |
| | p-value | 0.27 | 0.79 | 0.27 | 0.62 | 0.30 | 0.26 | 0.96 | 0.07 | 0.46 | 0.01 | 0.21 | 0.01 | 0.89 | 0.74 | 0.70 | 0.25 |
| | intercept (a) | 2261 | -27 | 2261 | 1398 | -56 | 100 | 11 | 472 | 306 | 933 | 748 | -461 | 177 | -43 | -57 | 130 |
| A5U | slope (b) | -0.71 | 0.04 | -0.71 | -0.47 | 0.01 | -0.02 | 0.02 | -0.19 | -0.09 | -0.41 | -0.23 | 0.14 | 0.04 | 0.00 | 0.04 | -0.02 |
| | p-value | 0.10 | 0.79 | 0.10 | 0.25 | 0.28 | 0.22 | 0.63 | 0.03 | 0.51 | 0.00 | 0.17 | 0.35 | 0.81 | 0.99 | 0.50 | 0.49 |
| | intercept (a) | 2522 | -32 | 2522 | 1863 | -26 | 51 | -38 | 435 | 243 | 980 | 737 | 46 | 100 | 23 | -79 | 50 |
| A5L | slope (b) | -0.34 | 0.12 | -0.34 | -0.09 | 0.07 | -0.03 | 0.05 | -0.18 | -0.22 | -0.13 | -0.35 | 0.58 | -0.19 | 0.05 | 0.08 | -0.07 |
| | p-value | 0.53 | 0.62 | 0.53 | 0.83 | 0.20 | 0.49 | 0.45 | 0.21 | 0.13 | 0.24 | 0.15 | 0.00 | 0.40 | 0.72 | 0.55 | 0.30 |
| | intercept (a) | 1635 | -157 | 1635 | 910 | -134 | 72 | -94 | 412 | 491 | 336 | 944 | -913 | 543 | -58 | -135 | 170 |
| A6 | slope (b) | -0.53 | 0.23 | -0.53 | -0.38 | 0.13 | 0.00 | 0.06 | -0.18 | -0.26 | -0.13 | -0.29 | 0.16 | -0.12 | 0.06 | 0.11 | -0.07 |
| | p-value | 0.34 | 0.47 | 0.34 | 0.33 | 0.18 | 0.97 | 0.38 | 0.16 | 0.08 | 0.04 | 0.12 | 0.38 | 0.56 | 0.65 | 0.49 | 0.54 |
| | intercept (a) | 1780 | -360 | 1780 | 1285 | -246 | 5 | -112 | 394 | 567 | 299 | 747 | -122 | 361 | -89 | -191 | 166 |

Appendix 6: Trend/slope (b), p-value, and Intercept (a) of rainfall for linear regression analysis: $y = a + bx$ where y is rainfall amount and x is time (2021-2100) in Amhara and its five Rainfall Regimes (A3-A6) for RCP 8.5 Scenario

| Place | Parameter | Annual | Bega | Belg | Kiremt | Jan | Feb | Mar | Apr | May | Jun | Jul | Aug | Sep | Oct | Nov | Dec |
|--------|---------------|--------|------|-------|--------|-------|-------|-------|-------|-------|-------|-------|-------|-------|------|------|------|
| Amhara | slope (b) | -1.53 | 0.44 | -1.53 | -1.75 | 0.00 | -0.01 | -0.02 | 0.02 | -0.21 | -0.49 | -0.91 | -0.09 | -0.27 | 0.24 | 0.17 | 0.02 |
| | p-value | 0.00 | 0.03 | 0.00 | 0.00 | 0.91 | 0.86 | 0.74 | 0.85 | 0.04 | 0.00 | 0.00 | 0.54 | 0.16 | 0.05 | 0.04 | 0.77 |
| | intercept (a) | 4181 | -810 | 4181 | 4436 | 20 | 24 | 55 | -6 | 482 | 1117 | 2104 | 486 | 729 | -466 | -333 | -31 |
| A3 | slope (b) | -2.68 | 0.33 | -2.68 | -2.34 | -0.01 | -0.03 | -0.06 | -0.02 | -0.55 | -0.71 | -1.14 | -0.23 | -0.27 | 0.09 | 0.25 | 0.00 |
| | p-value | 0.00 | 0.26 | 0.00 | 0.00 | 0.92 | 0.69 | 0.56 | 0.92 | 0.00 | 0.00 | 0.00 | 0.28 | 0.07 | 0.64 | 0.06 | 1.00 |
| | intercept (a) | 7081 | -554 | 7081 | 6048 | 26 | 86 | 167 | 111 | 1221 | 1667 | 2703 | 873 | 804 | -123 | -475 | 18 |
| A4 | slope (b) | -1.63 | 0.48 | -1.63 | -1.86 | 0.02 | 0.02 | -0.03 | 0.07 | -0.31 | -0.68 | -0.86 | -0.08 | -0.23 | 0.23 | 0.20 | 0.03 |
| | p-value | 0.00 | 0.02 | 0.00 | 0.00 | 0.69 | 0.63 | 0.67 | 0.61 | 0.01 | 0.00 | 0.00 | 0.56 | 0.21 | 0.09 | 0.01 | 0.71 |
| | intercept (a) | 4597 | -895 | 4597 | 4826 | -24 | -35 | 75 | -90 | 716 | 1549 | 2060 | 509 | 708 | -433 | -397 | -41 |
| A5U | slope (b) | -2.16 | 0.28 | -2.16 | -2.29 | 0.00 | 0.01 | 0.01 | 0.04 | -0.20 | -0.67 | -1.13 | -0.25 | -0.24 | 0.13 | 0.14 | 0.01 |
| | p-value | 0.00 | 0.05 | 0.00 | 0.00 | 0.83 | 0.80 | 0.88 | 0.68 | 0.07 | 0.00 | 0.00 | 0.09 | 0.25 | 0.19 | 0.01 | 0.80 |
| | intercept (a) | 5497 | -534 | 5497 | 5616 | 11 | -10 | -1 | -53 | 479 | 1511 | 2569 | 838 | 698 | -251 | -276 | -18 |

| Place | Parameter | Annual | Bega | Belg | Kiremt | Jan | Feb | Mar | Apr | May | Jun | Jul | Aug | Sep | Oct | Nov | Dec |
|-------|---------------|--------|-------|-------|--------|-------|-------|-------|-------|-------|-------|-------|-------|-------|------|------|------|
| A5L | slope (b) | -0.60 | 0.59 | -0.60 | -1.05 | 0.01 | -0.02 | -0.03 | 0.00 | -0.09 | -0.26 | -0.72 | 0.17 | -0.25 | 0.37 | 0.17 | 0.04 |
| | p-value | 0.21 | 0.01 | 0.21 | 0.02 | 0.90 | 0.63 | 0.68 | 0.99 | 0.35 | 0.00 | 0.00 | 0.35 | 0.29 | 0.01 | 0.11 | 0.63 |
| | intercept (a) | 2147 | -1121 | 2147 | 2883 | 2 | 56 | 82 | 33 | 215 | 597 | 1693 | -65 | 659 | -723 | -328 | -72 |
| A6 | slope (b) | -1.25 | 0.44 | -1.25 | -1.51 | -0.04 | -0.04 | -0.01 | -0.02 | -0.11 | -0.20 | -0.80 | -0.15 | -0.37 | 0.32 | 0.15 | 0.01 |
| | p-value | 0.00 | 0.11 | 0.00 | 0.00 | 0.61 | 0.53 | 0.88 | 0.86 | 0.30 | 0.00 | 0.00 | 0.49 | 0.06 | 0.03 | 0.23 | 0.91 |
| | intercept (a) | 3254 | -794 | 3254 | 3611 | 111 | 84 | 33 | 76 | 245 | 443 | 1790 | 513 | 865 | -619 | -282 | -4 |

Appendix 7: Near-term (2021-2040) average total rainfall amount in mm in three RCP scenarios in Amhara (A) and its five rainfall regimes (A3-A6)

| RCP 2.6 | | | | | | | RCP 4.5 | | | | | | RCP 8.5 | | | | | |
|---------|------|------|------|------|-----|-----|---------|------|------|------|-----|-----|---------|------|------|------|-----|-----|
| | A | A3 | A4 | A5U | A5L | A6 | A | A3 | A4 | A5U | A5L | A6 | A | A3 | A4 | A5U | A5L | A6 |
| Jan | 10 | 12 | 6 | 3 | 13 | 19 | 9 | 8 | 6 | 2 | 13 | 19 | 12 | 15 | 7 | 3 | 14 | 25 |
| Feb | 12 | 17 | 10 | 5 | 15 | 16 | 9 | 18 | 11 | 4 | 11 | 8 | 9 | 16 | 9 | 4 | 11 | 10 |
| Mar | 20 | 40 | 22 | 12 | 22 | 16 | 15 | 33 | 18 | 9 | 16 | 12 | 19 | 38 | 22 | 11 | 22 | 15 |
| Apr | 43 | 76 | 49 | 34 | 43 | 36 | 47 | 84 | 55 | 39 | 46 | 38 | 40 | 73 | 45 | 32 | 40 | 36 |
| May | 60 | 104 | 80 | 61 | 45 | 35 | 66 | 109 | 84 | 69 | 50 | 42 | 57 | 106 | 79 | 61 | 36 | 28 |
| Jun | 108 | 216 | 155 | 133 | 57 | 36 | 119 | 228 | 170 | 148 | 65 | 38 | 118 | 226 | 169 | 150 | 62 | 40 |
| Jul | 240 | 361 | 283 | 247 | 229 | 145 | 256 | 379 | 299 | 265 | 241 | 159 | 260 | 388 | 305 | 275 | 236 | 161 |
| Aug | 303 | 391 | 339 | 323 | 286 | 212 | 292 | 372 | 323 | 320 | 266 | 212 | 302 | 403 | 339 | 320 | 286 | 210 |
| Sep | 167 | 245 | 210 | 184 | 134 | 99 | 174 | 251 | 218 | 184 | 149 | 105 | 197 | 271 | 242 | 215 | 161 | 128 |
| Oct | 42 | 74 | 50 | 31 | 43 | 37 | 33 | 60 | 39 | 21 | 34 | 27 | 28 | 67 | 37 | 18 | 25 | 21 |
| Nov | 23 | 34 | 20 | 9 | 30 | 32 | 19 | 34 | 19 | 9 | 23 | 21 | 15 | 20 | 12 | 4 | 23 | 23 |
| Dec | 16 | 28 | 14 | 6 | 17 | 25 | 16 | 20 | 12 | 5 | 22 | 29 | 14 | 19 | 11 | 6 | 17 | 25 |
| Bega | 90 | 147 | 90 | 49 | 102 | 112 | 77 | 123 | 75 | 37 | 92 | 97 | 69 | 120 | 68 | 31 | 79 | 93 |
| Belg | 134 | 237 | 161 | 112 | 125 | 103 | 137 | 244 | 168 | 120 | 123 | 99 | 125 | 232 | 155 | 107 | 109 | 89 |
| Kiremt | 818 | 1213 | 986 | 886 | 707 | 492 | 840 | 1230 | 1009 | 916 | 721 | 514 | 877 | 1288 | 1054 | 959 | 744 | 540 |
| Annual | 1042 | 1597 | 1238 | 1047 | 933 | 708 | 1054 | 1596 | 1253 | 1074 | 936 | 710 | 1070 | 1640 | 1276 | 1098 | 932 | 722 |

Appendix 8: Mid-term (2041-2060) average total rainfall amount in mm in three RCP scenarios in Amhara (A) and its five rainfall regimes (A3-A6)

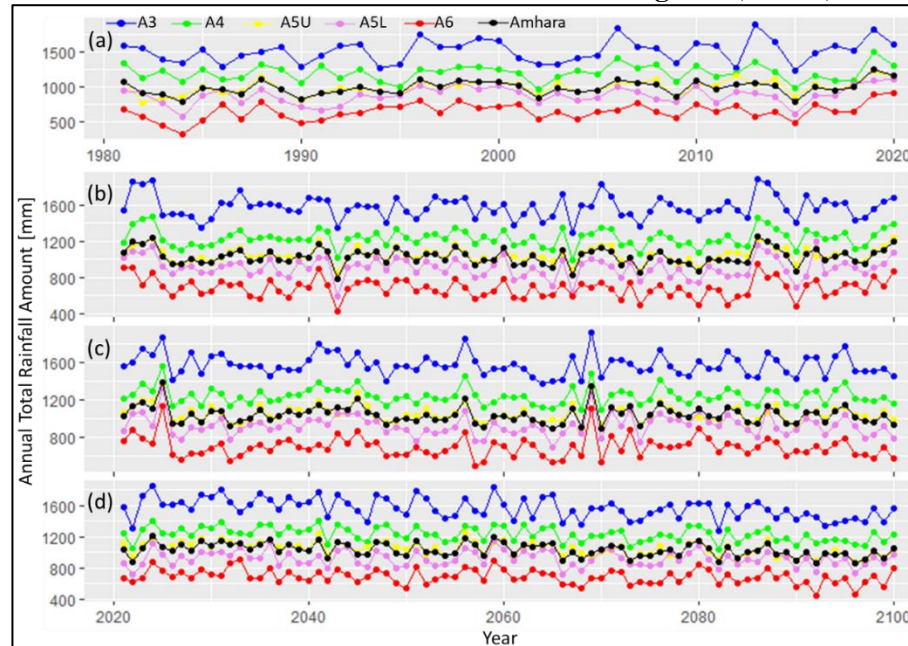
| RCP 2.6 | | | | | | | RCP 4.5 | | | | | | RCP 8.5 | | | | | |
|---------|-----|-----|-----|-----|-----|-----|---------|-----|-----|-----|-----|-----|---------|-----|-----|-----|-----|-----|
| | A | A3 | A4 | A5U | A5L | A6 | A | A3 | A4 | A5U | A5L | A6 | A | A3 | A4 | A5U | A5L | A6 |
| Jan | 9 | 7 | 4 | 2 | 14 | 21 | 8 | 4 | 3 | 1 | 12 | 19 | 11 | 9 | 6 | 2 | 15 | 22 |
| Feb | 7 | 8 | 6 | 2 | 11 | 10 | 8 | 10 | 7 | 3 | 10 | 10 | 10 | 16 | 9 | 5 | 13 | 14 |
| Mar | 14 | 30 | 17 | 10 | 14 | 11 | 19 | 39 | 21 | 13 | 18 | 15 | 20 | 38 | 22 | 11 | 24 | 16 |
| Apr | 44 | 76 | 50 | 36 | 43 | 38 | 43 | 82 | 52 | 37 | 41 | 29 | 38 | 66 | 42 | 30 | 38 | 30 |
| May | 57 | 98 | 77 | 63 | 41 | 29 | 54 | 96 | 74 | 59 | 36 | 29 | 59 | 108 | 81 | 64 | 38 | 30 |
| Jun | 113 | 221 | 159 | 134 | 65 | 40 | 112 | 219 | 160 | 135 | 63 | 38 | 109 | 215 | 156 | 136 | 57 | 34 |
| Jul | 252 | 379 | 298 | 260 | 235 | 153 | 244 | 373 | 292 | 249 | 228 | 147 | 248 | 379 | 292 | 257 | 229 | 152 |

| | RCP 2.6 | | | | | | RCP 4.5 | | | | | | RCP 8.5 | | | | | |
|--------|---------|------|------|------|-----|-----|---------|------|------|------|-----|-----|---------|------|------|------|-----|-----|
| | A | A3 | A4 | A5U | A5L | A6 | A | A3 | A4 | A5U | A5L | A6 | A | A3 | A4 | A5U | A5L | A6 |
| Aug | 304 | 390 | 344 | 323 | 288 | 211 | 306 | 408 | 346 | 329 | 286 | 205 | 307 | 395 | 345 | 328 | 291 | 214 |
| Sep | 174 | 249 | 222 | 188 | 142 | 105 | 174 | 251 | 220 | 190 | 140 | 104 | 178 | 254 | 224 | 202 | 139 | 103 |
| Oct | 37 | 77 | 47 | 23 | 36 | 30 | 38 | 68 | 46 | 27 | 38 | 34 | 39 | 73 | 46 | 29 | 38 | 31 |
| Nov | 17 | 27 | 16 | 7 | 20 | 21 | 19 | 31 | 19 | 8 | 25 | 25 | 24 | 32 | 20 | 10 | 32 | 34 |
| Dec | 10 | 12 | 6 | 3 | 14 | 21 | 18 | 27 | 15 | 6 | 22 | 32 | 14 | 17 | 10 | 4 | 19 | 25 |
| Bega | 73 | 123 | 73 | 35 | 84 | 94 | 84 | 130 | 82 | 43 | 97 | 109 | 87 | 131 | 83 | 46 | 104 | 112 |
| Belg | 123 | 211 | 150 | 111 | 110 | 87 | 124 | 227 | 155 | 112 | 105 | 83 | 126 | 228 | 155 | 110 | 113 | 91 |
| Kiremt | 842 | 1238 | 1022 | 905 | 730 | 508 | 835 | 1251 | 1018 | 902 | 717 | 495 | 842 | 1242 | 1017 | 923 | 716 | 503 |
| Annual | 1037 | 1572 | 1245 | 1051 | 923 | 689 | 1042 | 1608 | 1255 | 1057 | 919 | 686 | 1054 | 1600 | 1254 | 1079 | 932 | 707 |

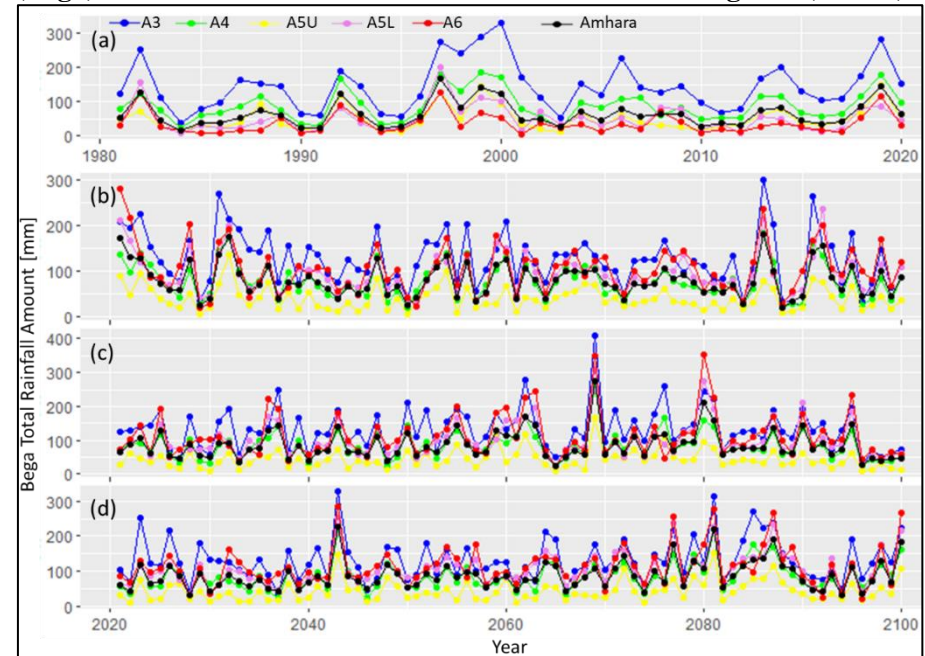
Appendix 9: Long-term (2061-2100) average total rainfall amount in mm in three RCP scenarios in Amhara (A) and its five rainfall regimes (A3-A6)

| | RCP 2.6 | | | | | | RCP 4.5 | | | | | | RCP 8.5 | | | | | |
|--------|---------|------|------|------|-----|-----|---------|------|------|------|-----|-----|---------|------|------|-----|-----|-----|
| | A | A3 | A4 | A5U | A5L | A6 | A | A3 | A4 | A5U | A5L | A6 | A | A3 | A4 | A5U | A5L | A6 |
| Jan | 11 | 12 | 7 | 4 | 14 | 24 | 12 | 9 | 7 | 3 | 16 | 26 | 12 | 15 | 10 | 4 | 16 | 22 |
| Feb | 11 | 20 | 11 | 5 | 14 | 13 | 7 | 12 | 8 | 2 | 9 | 8 | 9 | 15 | 11 | 4 | 11 | 10 |
| Mar | 25 | 43 | 26 | 12 | 34 | 23 | 19 | 35 | 21 | 13 | 22 | 18 | 19 | 38 | 22 | 13 | 22 | 15 |
| Apr | 53 | 88 | 58 | 45 | 51 | 49 | 37 | 69 | 45 | 30 | 36 | 28 | 40 | 69 | 47 | 33 | 38 | 32 |
| May | 65 | 112 | 86 | 72 | 44 | 34 | 52 | 92 | 71 | 59 | 34 | 25 | 43 | 73 | 60 | 48 | 30 | 20 |
| Jun | 100 | 206 | 145 | 125 | 49 | 28 | 104 | 214 | 151 | 127 | 56 | 32 | 87 | 183 | 125 | 108 | 44 | 27 |
| Jul | 260 | 385 | 308 | 274 | 236 | 161 | 241 | 368 | 289 | 249 | 223 | 143 | 202 | 316 | 248 | 206 | 186 | 113 |
| Aug | 303 | 387 | 339 | 330 | 284 | 209 | 316 | 411 | 353 | 332 | 306 | 219 | 295 | 384 | 332 | 304 | 295 | 201 |
| Sep | 158 | 243 | 208 | 176 | 121 | 79 | 170 | 250 | 220 | 190 | 131 | 97 | 175 | 248 | 223 | 198 | 138 | 102 |
| Oct | 32 | 60 | 39 | 20 | 32 | 26 | 34 | 65 | 41 | 19 | 37 | 31 | 44 | 74 | 52 | 29 | 47 | 40 |
| Nov | 19 | 28 | 17 | 6 | 26 | 24 | 20 | 29 | 19 | 9 | 26 | 25 | 27 | 38 | 26 | 14 | 35 | 34 |
| Dec | 15 | 14 | 9 | 6 | 20 | 32 | 12 | 13 | 8 | 4 | 17 | 25 | 18 | 24 | 16 | 8 | 23 | 29 |
| Bega | 76 | 114 | 72 | 36 | 92 | 106 | 78 | 116 | 74 | 35 | 97 | 107 | 102 | 151 | 103 | 54 | 121 | 124 |
| Belg | 154 | 263 | 182 | 134 | 142 | 118 | 116 | 208 | 145 | 103 | 101 | 79 | 112 | 195 | 140 | 98 | 101 | 77 |
| Kiremt | 820 | 1221 | 1001 | 904 | 690 | 477 | 832 | 1242 | 1014 | 898 | 716 | 491 | 760 | 1131 | 928 | 816 | 662 | 442 |
| Annual | 1050 | 1598 | 1255 | 1073 | 924 | 701 | 1026 | 1566 | 1233 | 1037 | 914 | 677 | 973 | 1476 | 1171 | 968 | 885 | 644 |

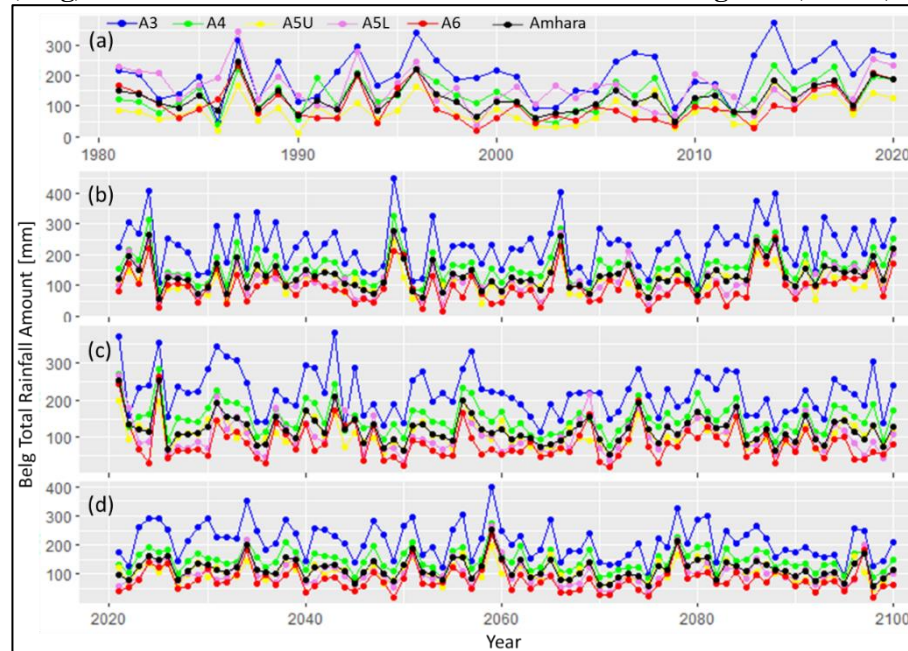
Appendix 10: Time series of historical (1981-2020) (a) and future (2021-2100) for RCP 2.6 (b), RCP 4.5 (c), and RCP 8.5 (d) Scenarios annual total rainfall amount in Amhara and its Rainfall Regimes (A3-A6)



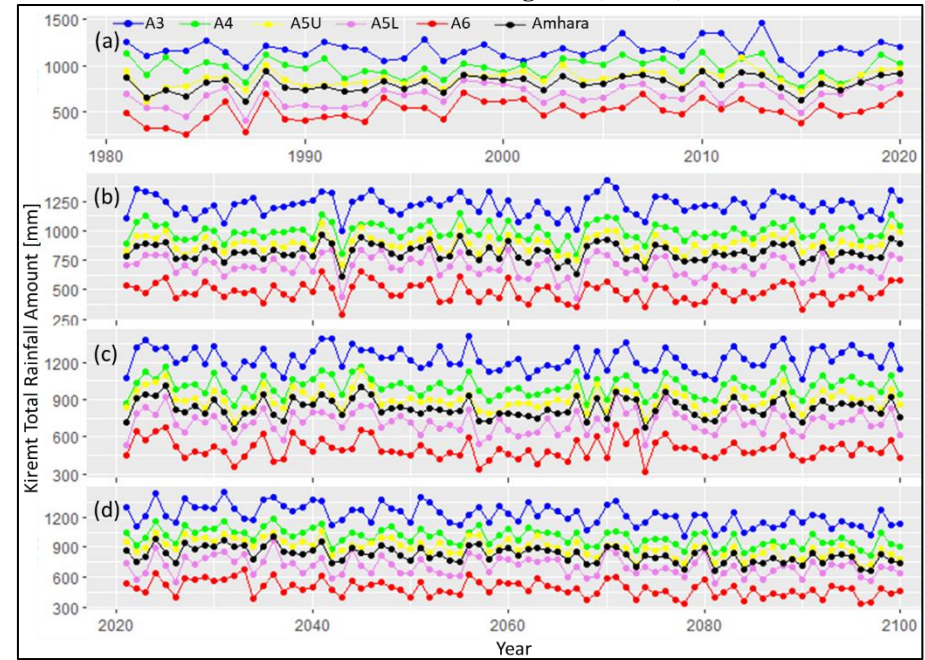
Appendix 11: Time series of historical (1981-2020) (a) and future (2021-2100) for RCP 2.6 (b), RCP 4.5 (c), and RCP 8.5 (d) Scenarios Oct-Jan (Bega) total rainfall amount in Amhara & its Rainfall Regimes (A3-A6)



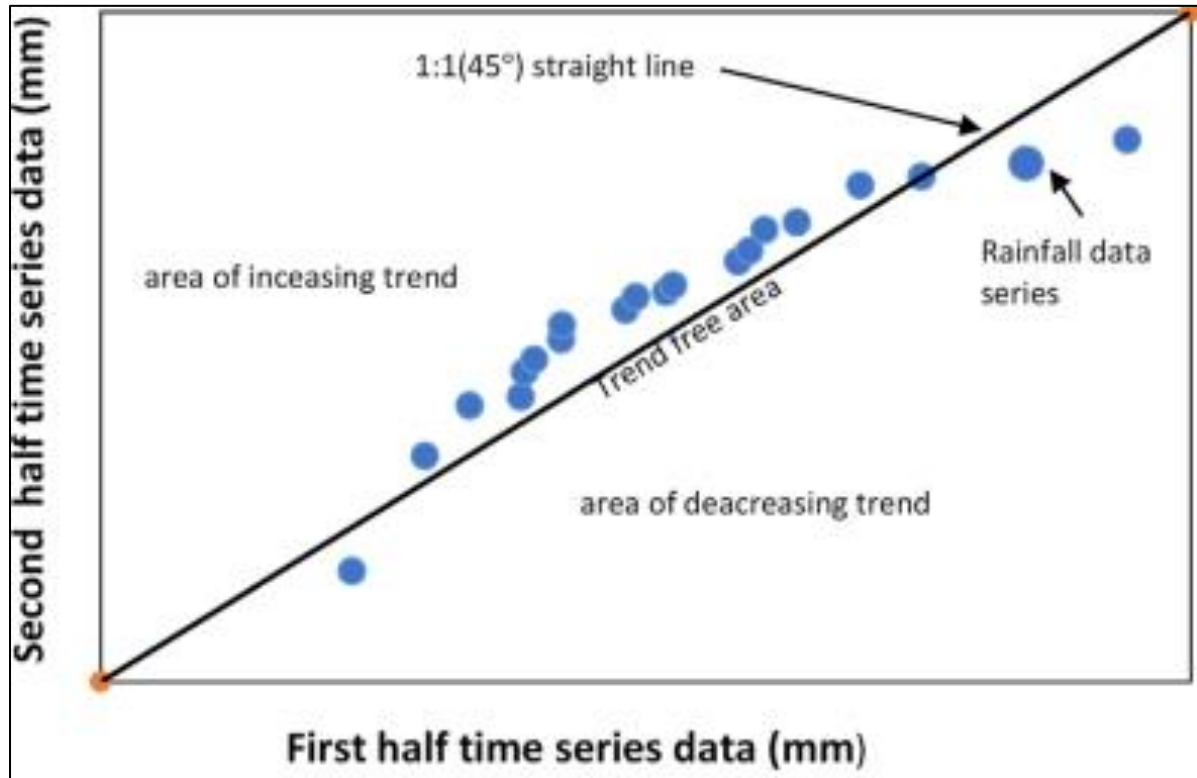
Appendix 12: Time series of historical (1981-2020) (a) and future (2021-2100) for RCP 2.6 (b), RCP 4.5 (c), and RCP 8.5 (d) Scenarios Feb-May (Belg) total rainfall amount in Amhara & its Rainfall Regimes (A3-A6)



Appendix 13: Time series of historical (1981-2020) (a) and future (2021-2100) for RCP 2.6 (b), RCP 4.5 (c), and RCP 8.5 (d) Scenarios Jun-Jul (Kiremt) total rainfall amount in Amhara & its Rainfall Regimes (A3-A6)



Appendix 14: Innovative trend analysis methodology template



Source: (Terefe et al., 2022)